

**ANALYSIS OF MAGNETIC RESONANCE IMAGING
FEATURES OF VIRCHOW-ROBIN SPACES ASSOCIATED
WITH CEREBRAL SMALL VESSEL DISEASE**

A thesis in partial fulfilment of the requirements of Master of Science Degree in Human
Anatomy, University of Nairobi:

Dr. Brian Ngure Kariuki

H56/36539/2020

July 2023

Department of Human Anatomy,

University of Nairobi,

P.O. Box 30197-00100,

NAIROBI.

DECLARATION

I hereby confirm that this dissertation is my original work and has not been presented elsewhere for examination:

Sign: 

Date: 04/07/2023

Dr Brian Ngure Kariuki, Bsc, MBChB.

H56/36539/2020

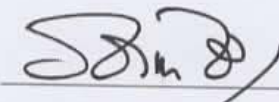
This proposal is being submitted with our approval as university supervisors:

1. Sign:  Date: 05-07-23

Dr Paul Odula, BSc, MBChB, MMED (Surgery), PhD.

Senior Lecturer, Department of Human Anatomy, University of Nairobi

odula@uonbi.ac.ke +254722773025

2. Sign:  Date: 04/07/2023

Prof. Obimbo Moses Madadi, MBChB, Dip FELASA C, MSc, MMED (ObGyn), PhD.

Associate Professor, Department of Human Anatomy, University of Nairobi

moses.obimbo@uonbi.ac.ke +254721585906

3. Sign:  Date: 04th July 2023

Dr. Pamela Mandela, MBChB, MPH, MMED (ENT), PhD.

Senior Lecturer, Department of Human Anatomy, University of Nairobi

pamela.idenya@uonbi.ac.ke +254724277070

Funding support

This study was supported by a Kenyatta National Hospital grant, reference number KNH/R&P/23K/41/6.

DEDICATION

How very quietly you tiptoed into our world, silently, only a moment you stayed.

But what an imprint your footsteps have left upon our hearts.

ACKNOWLEDGEMENT

I would like to sincerely thank my Creator, who has made this dream true.

I most sincerely extend my deepest gratitude to my supervisors and academic mentors, Professor Moses Obimbo and Drs. Paul Odula, Pamela Mandela, Beda Olabu, and Eunice Omamo. Your support and guidance during the development of this study has been immeasurable.

I appreciate the guidance offered to me by the late Prof. Hassan Saidi, Prof. Julius Ogeng'o, and Drs. Bernard Ndung'u, James Kigera, and Jeremiah Munguti. Your astute guidance has shaped my scientific journey.

To my friends, Drs. Musa Misiani, Isaac Cheruiyot, Vincent Kipkorir, and Talha Mohammed, and all my friends in the BSc Anatomy classes of 2020 and 2021. This road less traveled has been illuminated by your acute intellect.

My deepest gratitude to my colleagues: Drs. Wanjiku Ndung'u, Barasa Wafula, Musa Misiani, Raymond Kebaso, Nick Ndemange, and Ms Mercy Sing'oei, you truly made this remarkable academic journey a memorable one.

To the technical staff at the Department of Human Anatomy and the Department of Radiology (KNH), you have been excellent guides who have turned the concepts herein into tangible results.

To the KNH medical research department, you have offered financial and technical support. The scheduled progress meetings also ensured the study ran smoothly.

My wife Sindo and daughter Nala, thank you for your patience and undying affection even as I worked to complete this thesis.

TABLE OF CONTENTS

Declaration	i
Dedication	iv
Acknowledgement	v
Table of Contents	vi
List of abbreviations	viii
Operational definitions.....	x
List of figures	x
List of tables.....	xi
Summary of the Thesis	1
Chapter One: Introduction and Literature Review.....	2
1.1 Introduction.....	2
1.2 Literature Review.....	5
1.2.1 Structure and functions of Virchow-Robin spaces.....	6
1.2.2 MRI morphology and morphometry of Virchow-Robin spaces in CSVDand NCSVD	9
1.2.3 Association between MRI features of Virchow-Robin spaces and CSVD	12
1.2.4 Predictive features of CVSD using MRI analysis Virchowhow-Robin spaces.....	14
1.3 Significance of the Study	16
1.4 Study Justification.....	16
1.5 Conceptual Framework.....	17
1.6 Study Question.....	19
1.7 Hypothesis.....	19
1.8 Objectives	19
1.8.1 Broad objective	19
1.8.2 Specific objectives	19
Chapter Two: Materials And Methods	20
2.1 Study Design.....	20
2.2 Study Area And Site Description.....	20
2.3 Study Population.....	21
2.3.1 Inclusion criteria	21
2.3.2 Exclusion criteria	21
2.4 Sample Size Calculation	22
2.5 Screening, Recruitment, Enrollment and Consenting Procedures	23

2.6 Variables	24
2.7 Image Acquisition and Data Collection Procedures	24
2.8 Quality Assurance Procedures	28
2.9 Ethical Considerations	28
3.0 Data Analysis Plan	29
Chapter Three: Results.....	30
3.1 Demographics of Study Study Subjects.....	30
3.2 MRI Morphology and Morphometry of Virchow-Robin Spaces in CVSD and NCVSD	31
3.3 Association between MRI Features of Virchow-Robin Spaces and CVSD	34
3.4 Predictive Features of CVSD using MRI Analysis of Virchow-Robin Spaces	35
Chapter Four: Discussion and Conclusion.....	38
4.1 Demographic, Comorbidities and Social Characteristics	38
4.2 MRI Morphology and Morphometry of Virchow-Robin Spaces In CVSD and NVSD	41
4.3 Association between MRI Features Of Virchow-Robin Spaces And CVSD	43
4.4 Predictive Features of CVSD Using MRI analysis Of Virchow-Robin Spaces	46
Conclusion	47
Recommendations:	47
Suggestions for Further Studies:.....	47
Study Limitations and Delimitations	48
Study Limitations.....	48
Study Delimitations	48
References.....	49
Appendices.....	i
Appendix I: Data Collection Tool.....	i
Appendix II: Participant Information and Consent Form	iii
English Informed Consent Form.....	iii
Kiswahili Informed Consent Form	ix

LIST OF ABBREVIATIONS

AQP4	Aquaporin-4
AUC	Area under the curve
BBB	Blood-brain barrier
CAA	Cerebral amyloid angiopathy
CADASIL	Cerebral autosomal dominant arteriopathy with subcortical ischemic strokes and leukoencephalopathy
COVID-19	Coronavirus disease 2019
CSF	Cerebrospinal Fluid
CSVD	Cerebral small vessel disease
DPA	Deep Perforating Arteriopathy
dWMH	Deep white matter hyperintensities
EPVS	Enlarged perivascular spaces
FLAIR	Fluid-attenuated inversion recovery
FOV	Field-of-view
GLS	Glymphatic system
HC	Healthy controls
ISF	Interstitial Fluid
KNH/UON/ERC Kenyatta National Hospital University of Nairobi Ethics and Research Committee	
MI	Myocardial infarction
MRI	Magnetic resonance imaging
NCSVD	Non cerebral small vessel disease
NVC	Neurovascular coupling
NVU	Neurovascular unit
PVH	Periventricular white matter hyperintensities
PVS	Perivascular (Virchow-Robin) spaces
ROC	Receiver operating characteristic

SPSS	Statistical package for social sciences
STRIVE	Standards for Reporting Vascular changes on Neuroimaging
T1w	T1-weighted
T2w	T2- weighted
TIA	Transient ischemic attack
VSMC	Vascular smooth muscle cells
WMH	White matter hyperintensities

OPERATIONAL DEFINITIONS

Cerebral small vessel disease: a diverse collection of neuropathological changes with resultant clinical and neuroimaging findings that affect minute perforating arteries, arterioles, capillaries, and venules hence causing cerebral white matter and deep grey matter damage.

Virchow-Robin spaces: also known as perivascular spaces. These are cerebrospinal fluid-filled invaginations of the subarachnoid space that surround small penetrating cerebral arterioles as they course into the brain parenchyma.

LIST OF FIGURES

Figure 1 Pictorial representation of Virchow Robin Space	8
Figure 2 MR image showing Virchow Robin spaces	11
Figure 3 Conceptual Framework	18
Figure 4 Findings on MRI for lesions related to CSVD	25
Figure 5 Visual rating of Virchow-Robin spaces as described by Potter et al., EPVS – Enlarged Virchow-Robin spaces (2015).	26
Figure 6 Grading of white matter hyperintensities using the Fazekas scale (Qu et al., 2020). HC – healthy controls with no white matter hyperintensities (WMH).	27
Figure 7 A schematic illustration of measurement of individual Virchow-Robin space to obtain the L –length, W – width or diameter and Virchow-Robin space area/size	28
Figure 8 Graph comparing Virchow-Robin space features between CSVD and NCSVD groups.	33
Figure 9 ROC curves of quantitative features of Virchow-Robin spaces for predicting CSVD ..	37

LIST OF TABLES

Table 1 A comparative analysis of demographic, medical comorbidities and social characteristics of study study subjects	30
Table 2 Difference in the morphology of PVS between CSVD and NCSVD groups	31
Table 3 Crude and adjusted odds ratio of factors predictive of CSVD.	35

SUMMARY OF THE THESIS

Background: A critical component of the radiological diagnosis of cerebral small vascular disease (CSVD) is magnetic resonance imaging (MRI). Subcortical infarcts, microbleeds, lacunes, and white matter hyperintensities (WMH), which are all late signs of the disease, are imaging characteristics that are considered diagnostic. Virchow-Robin spaces have been identified as potential early biomarkers of CSVD. However, there is still a lack of clarity in their association yet this is important in gaining insight into the mechanistic process of cerebral small vascular disorders and the design of potential targeted therapies. Thus, the goal of this study was to examine the MRI characteristics of CSVD-related Virchow-Robin space features.

Materials and methods: Magnetic resonance images of study subjects with clinical and supporting radiologic features of CSVD were obtained. Age and sex-matched images, from study subjects with no clinical or radiologic features of CSVD, were used for comparison. Data collected included age, sex, history of alcohol consumption, smoking, medical comorbidities (hypertension and diabetes), absolute count of Virchow-Robin spaces, their anatomic location, length, diameter, area and white matter hyperintensities– using Fazekas scale.

Data management: Independent student's T-test was used to compare age, substance use, morphometric characteristics and the total white matter hyperintensity burden score. The association between sex, comorbidities, substance use and anatomic location were measured using crude and adjusted odds ratio in univariate and multivariate analysis respectively. Receiver operating characteristic analysis was used to obtain the specificity and sensitivity for each variable.

Results: In the study, 118 study subjects were included, with 43 (36%) diagnosed with CSVD. The CSVD group was significantly older (55.1 ± 19.0 vs 44.9 ± 16.4 years, $p=0.003$), and had higher prevalence of hypertension (OR=9.3, 95% CI 9.1-9.3, $p<0.001$) and diabetes (OR=9.8, 95% CI 7.3-13.3, $p<0.001$) than the non-CSVD group. CSVD study subjects had a greater number of Virchow-Robin spaces (28.5 ± 11.2 vs 12.2 ± 8.5 , $p<0.001$), higher Potter's rating scale scores ($p<0.001$), and more frequent type 3 location ($p=0.007$), periventricular hyperintensities ($p=0.005$), deep white matter hyperintensities ($p=0.001$), and total white matter hyperintensity burden score ($p=0.001$). They also had wider (2.4 ± 0.9 vs 1.7 ± 0.7 mm, $p<0.001$), longer (2.4 ± 0.8 vs 1.9 ± 0.7 mm, $p<0.001$), and larger area (18.4 ± 10.9 vs 11.5 ± 6.5 mm², $p<0.001$).

Conclusion: MRI features associated with CSVD include: a high Potter's scale, a high frequency of type III Virchow-Robin spaces, larger Virchow-Robin spaces and a high absolute count of Virchow-Robin spaces. The absolute number of Virchow-Robin spaces provided the best prediction model for CSVD, with the highest sensitivity and specificity, in comparison to the routinely used total white matter hyperintensity burden score.

CHAPTER ONE: INTRODUCTION AND LITERATURE REVIEW

1.1 INTRODUCTION

Virchow-Robin spaces, also referred to as perivascular spaces (PVS), are subarachnoid space invaginations filled with cerebrospinal fluid (CSF) that course into the brain parenchyma (Reith and Haußmann, 2018; Zhang et al., 1990). Before the advent of MRI, these spaces were only demonstrable on autopsy/biopsy sections (Braffman et al., 1988). Virchow-Robin spaces and their enclosed vessels are often seen as single vessel-like structures on T2-weighted brain MRI scans. They appear as distinctive minute high-signal regions in the basal ganglia, anterior perforated substance, midbrain and centrum semiovale and are in similar alignment to penetrating arterioles (Doubal et al., 2010; Song et al., 2000). Their appearance on brain sections is linear on coronal plane images and dot-like, ovoid or curvilinear on transverse plane images.

Small Virchow-Robin spaces appear in all age groups. Typically measuring less than 2 millimetres (mm) in diameter (Heier et al., 1989). However, histopathological findings have proposed a positive correlation between age and morphometric properties of Virchow-Robin spaces (Pesce and Carli, 1988). In relation to their spatial distribution in the brain, the location of these spaces correlates to that of perforating arterioles entering the medial temporal lobe, corpus striatum and thalamus and this pattern is consistent on MRI (Jungreis et al., 1988).

Various researchers have categorized Virchow-Robin spaces into type I, type II and type III corresponding to the location of the perforating arteries (Jungreis et al., 1988; Rudie et al., 2018a; Kwee & Kwee, 2007;). Lenticulostriate arteries coexist with Type I Virchow-Robin spaces. Within the midbrain, Type II Virchow-Robin gaps are seen accompanying perforating medullary arteries as they pass through cortical gray matter with high convexities and extend into the white matter.

Type III Virchow-Robin spaces are located at the ponto-mesencephalic intersection of the brainstem encircling the penetrating collicular and accessory collicular artery branches (Heier et al., 1989; Rudie et al., 2018; Jungreis et al., 1988; Kwee)

Cerebral small vessel diseases (CSVD) vary largely in causation mechanisms but share a similar pattern of pathology. Their characteristics include distended Virchow-Robin spaces. (Mestre et al., 2017). Medical comorbidities, inclusive of diabetes mellitus, hypertension, as well as recreational drug use, especially alcohol abuse and cigarette smoking are known to cause macrovascular and microvascular changes (Gons et al., 2011; Chawla et al., 2016; Brown et al., 2018). These have been implicated in some changes observed in the cerebral vasculature as well as disordered drainage of the glymphatic system. These effects may underpin the changes observed in the morphometry and morphology of Virchow-Robin spaces (Debette et al., 2011; Power et al., 2017).

CSVD presents a challenge in vivo detection. Clinicians often are forced to count on imaging markers, predominantly a combination of periventricular white matter hyperintensities, microbleeds and lacunes that compose the band of CSVD. These late imaging indicators are often identified accompanied by significant symptomatology such as cognitive deterioration, features of stroke, as well as other neuropsychiatric disorders (Mestre et al., 2017; Moran et al., 2012). Enlarged Virchow-Robin spaces located in the brain are an essential neuroimaging marker of vascular alterations in the brain, particularly the pathophysiology of CSVD (Doubal et al., 2010). Recent discoveries term enlarged Virchow-Robin spaces as potential early biomarkers of CSVD (Charidimou et al., 2016). However, from the current literature reviewed there is paucity of information on the association between enlarged Virchow-Robin spaces and CSVD.

Virchow-Robin spaces, visible on MRI scans, have for long been thought to be artefactual. Now they are described as unique biomarkers for CSVD and related brain disorders which have a vascular component (Brown et al., 2018). As such, an in-depth characterization of Virchow-Robin spaces and their association with CSVD could offer a reliable approach for the early diagnosis of CSVD. However, there is limited knowledge about the role of anatomical variations and their association with the occurrence of CSVD (Mestre et al., 2017). From the current literature reviewed there is paucity of information on the contrast in the MRI features of Virchow-Robin spaces in CSVD compared to age-matched healthy study subjects. An understanding of the anatomy of Virchow-Robin spaces and the effects of CSVD may be useful in the identification patterns that will serve as indices for early detection of Virchow-Robin space or vascular-related changes in patients having neurological conditions such as CSVD. In addition, the findings may be useful in developing a predictive diagnostic model for CSVD.

1.2 LITERATURE REVIEW

CSVD is a chronic progressive disease of arterioles, capillaries and small veins supplying the white matter and deep nuclei of the brain. It affects small vessels between 50-400 micrometres in diameter. CSVD occurs six to ten times more often than stroke. Theoretically, approximately 25% of individuals more than 80 years have had a silent infarct, which is the most identified incidental finding on neuroimaging. This condition is responsible for 20% of all strokes and 45% of all vascular dementias. Neuroimaging and neuropathological studies of the brain reveal substantial differences in the clinical picture of CSVD. Currently, neuroimaging using MRI is the diagnostic gold standard.

Virchow-Robin spaces are defined as subarachnoid space extensions that edge small penetrating cerebral arterioles. Virchow-Robin spaces are named after two prominent figures in medical history. Rudolf Virchow, a German physician and pathologist, who first described these spaces in 1859 and Henri Pierre Marie Robin, a French anatomist. Rudolf Virchow observed them as perivascular spaces surrounding blood vessels in the brain. Jean-Martin Charcot, a French neurologist, further investigated these spaces and provided detailed anatomical descriptions. However, it was Henri Pierre Marie Robin who is credited with the definitive description of these spaces in 1923. Virchow-Robin spaces are defined as subarachnoid space extensions that edge small penetrating cerebral arterioles.

Before the discovery of MRI, the significance of Virchow-Robin spaces was limited due to the lack of non-invasive imaging techniques. Their presence was mainly noted during autopsies and histological examinations. These spaces were considered as potential routes for the spread of infections or tumors in the brain, as they offered a path for fluid or cellular elements to travel within the brain tissue. With MRI, researchers and clinicians gained a better understanding of the

anatomical distribution, characteristics, and pathologies associated with these spaces. Virchow Robin spaces exhibit varying anatomical characteristics which are potentially useful in predicting occurrence of CSVD.

1.2.1 Structure and functions of Virchow-Robin spaces

Virchow-Robin spaces are conventionally defined as fluid-filled subarachnoid invaginations which encircle small perforating cerebral microvessels, during their intra-parenchymal course (Ballerini, Booth, Valdés Hernández, et al., 2020). Within these spaces, the respective microvessels are surrounded by perivascular macrophages as well as fibroblastic cells. They are characterized by sieve-like perforations, separated from the subarachnoid space by pial flattened cells in their course to reflect onto the cerebral microvessels. (Mestre et al., 2017; Zhang et al., 1990). Virchow-Robin spaces are therefore lined externally by the pia matter and internally by aquaporin-4 (AQP4) associated astrocytic end-feet which abut the ad-luminal vessel wall (Fanous and Midia, 2007). While they have no direct connection with the subarachnoid space, they are known to communicate with the subpial space and also extend distally as far as the capillaries where they form fenestrations. This results in the fusion of vascular and glial components causing obliteration of the space between them. As a result, subpial complimentary venules lack the continuity of the perivascular sheath observed on the arteriole side (Woldenberg and Kohn, 2014).

Perivascular spaces called Virchow-Robin spaces surround blood vessels as they enter the brain matter from the subarachnoid region. CSF is present in these gaps, which are bordered with pia mater. Their main job is to act as a conduit for immune cells and fluid between the brain parenchyma and the subarachnoid space. Contrarily, fluid-filled regions known as perivascular spaces surround blood arteries as they travel through the brain. They are surrounded by glial cells and are situated within the brain parenchyma. In perivascular spaces, waste clearing and chemical

exchange between blood vessels and the surrounding brain tissue occur. While perivascular spaces are more directly involved in the exchange of chemicals between blood arteries and brain tissue, Virchow-Robin spaces primarily serve as CSF conduits. Both structures are crucial to the fluid dynamics of the brain.

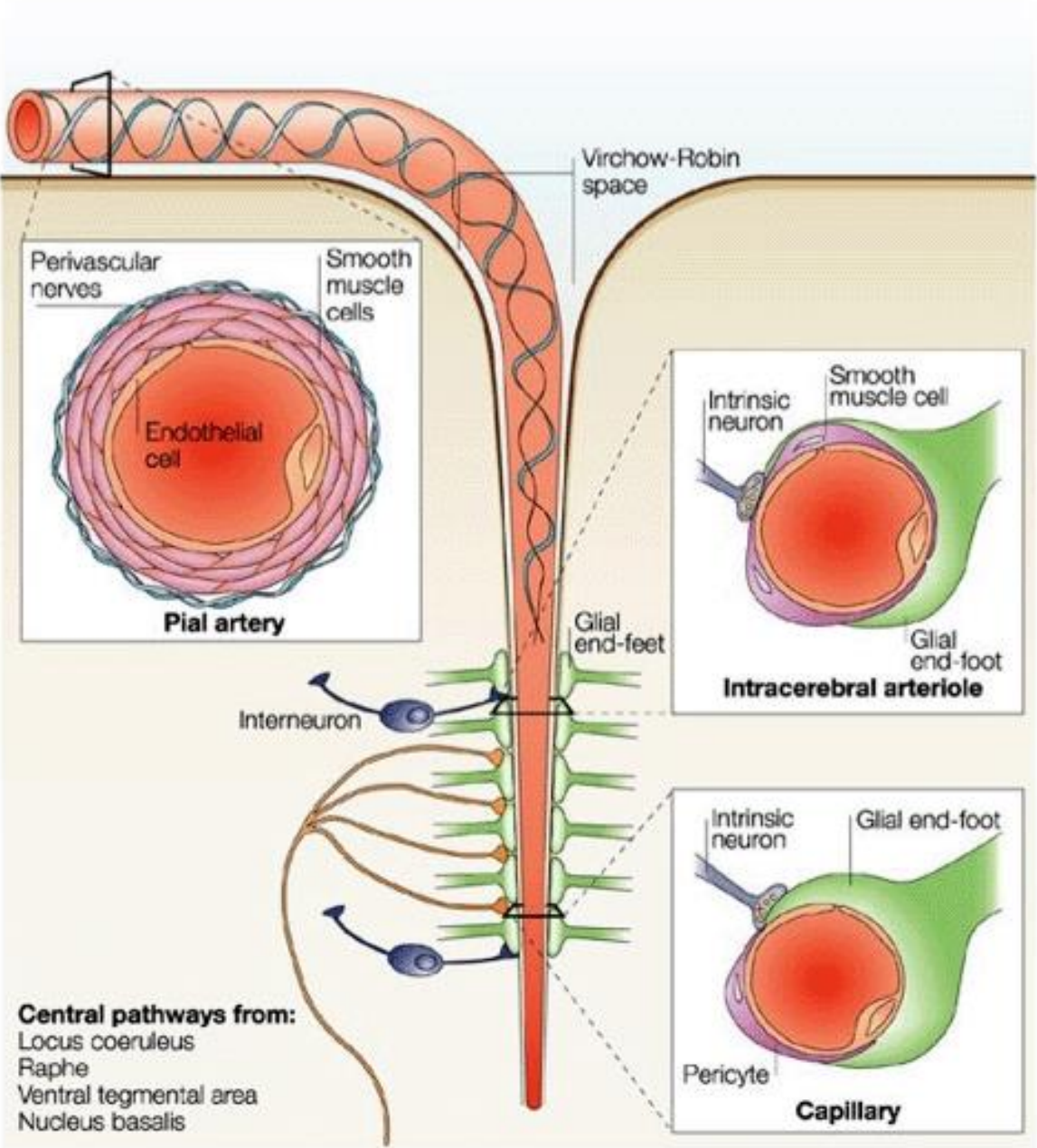
Virchow-Robin spaces are integral in the transport of fluids within the brain compartments and enhance waste product clearance (Brown et al., 2018). These diversely connected Virchow-Robin spaces are lined by aquaporin-4 (AQP4) associated astrocytic end feet and form a fundamental part of the glymphatic system (GLS). The GLS is a pathway that consistently confers fluid exchange between CSF and ISF compartments, depending on body posture and the sleep-wake cycle (Mestre et al., 2017).

Influx of CSF into the periarterial spaces is important for glucose delivery, transportation of signaling molecules and lipids as well as choroid plexus derived apolipoprotein E across the brain. Glymphatic efflux, on the other hand, facilitates the clearance of waste products and solutes (Acharyar et al., 2016). Patency of the GLS has been described as a crucial indicator of normal brain function (Louveau et al., 2015). To this end, the structural and functional integrity of Virchow-Robin spaces is considered key in the maintenance of normal homeostatic control of glymphatic function, especially as regards the role of Virchow-Robin space AQP4 polarization (Thrane et al., 2013).

Failure of the glymphatic bulk flow, as observed in vascular remodelling, enlargement of Virchow-Robin spaces, as well as perivascular collection of β -amyloid and granular osmiophilic material in cerebral small vessel disease, affects bulk flow and hence may present as different pathological states (Mestre et al., 2017). Imaging of Virchow-Robin spaces may hence provide useful insights

into the organization of the glymphatic system in both physiological and pathological states (Zong et al., 2016).

Figure 1: Pictorial representation of a Virchow Robin Space (Virchow-Robin_space [Neurosurgery Wiki], 2021)



Nature Reviews | Neuroscience

1.2.2 MRI morphology and morphometry of Virchow-robin spaces in CSVD and NCSVD

Before the discovery of MRI, Virchow-Robin spaces were only visualized on autopsy and biopsy sections of the basal ganglia or white matter. They often demonstrated no ostensible alteration in their immediate parenchymal tissue but were at times associated with a narrow border of fibrillary gliosis or pale, sinuous myelin sheaths (Braffman et al., 1988). With the advent of high-spatial-resolution MRI, they are currently visualized on T2- or T1-weighted sequences, especially when enlarged, as a single vessel-like complex. They appear distinctively as small high-signal areas, with similar attenuation as CSF on all pulse sequences, often either in clusters of several, contiguous, well-defined parenchymal cysts of different sizes or as a large solitary parenchymal cyst.

Virchow Robin Spaces are regularly detected within the basal ganglia, anterior perforated substance, midbrain, sub-insular regions, dentate gyrus and centrum semiovale, following penetrating arterioles alignment (Doubal et al., 2010; Song et al., 2000). On Fluid-attenuated inversion recovery (FLAIR) scans, fluid within Virchow-Robin spaces appear completely suppressed, neither exhibiting restricted diffusion nor enhancing after administration of contrast except in the presence of invasive pathologies. Axial MRI sections depict Virchow-Robin spaces as sharply demarcated dot-like, ovoid or curvilinear fluid-filled cysts, while oriented linearly on coronal plane MRI images. Variations in location, morphology and symmetry of Virchow-Robin spaces have been observed (Rudie et al., 2018b)

Small Virchow-Robin spaces (< 2 mm) are regarded as anatomical variants in normal individuals. They are seen in approximately 13% to 76% of adults. On MRI, they appear as small foci measuring < 2 mm in cross-sectional diameter, dilated when >5mm, and can expand and enlarge

with extremes of up to >1.5cm in size where they are referred to as giant Virchow-Robin spaces (Pesce and Carli, 1988). While dilated Virchow-Robin spaces are observed in about 1.6% to 3% of healthy individuals, histopathological findings suggest a positive correlation between Virchow-Robin space dimensions and age (Rudie et al., 2018).

Virchow-Robin spaces have been stratified into 3 types based on the location of their associated vessels (Rudie et al., 2018). As such, type I Virchow-Robin spaces circumscribe lenticulostriate vessels as they traverse the anterior-perforated substance to enter into basal ganglia. Medullary arteries are encircled by Type II Virchow-Robin gaps when they pass through high convexities of the cortex gray matter and into the cortex white matter. Type III Virchow-Robin spaces are found at the ponto-mesencephalic intersection of the brainstem encircling the penetrating collicular and accessory collicular artery branches. However, these spaces can be identified all through the infratentorial and supratentorial regions of the brain where vessels exist (Rudie et al., 2018). Further, morphologic, morphometric and spatial characteristics of Virchow-Robin spaces remain variable.

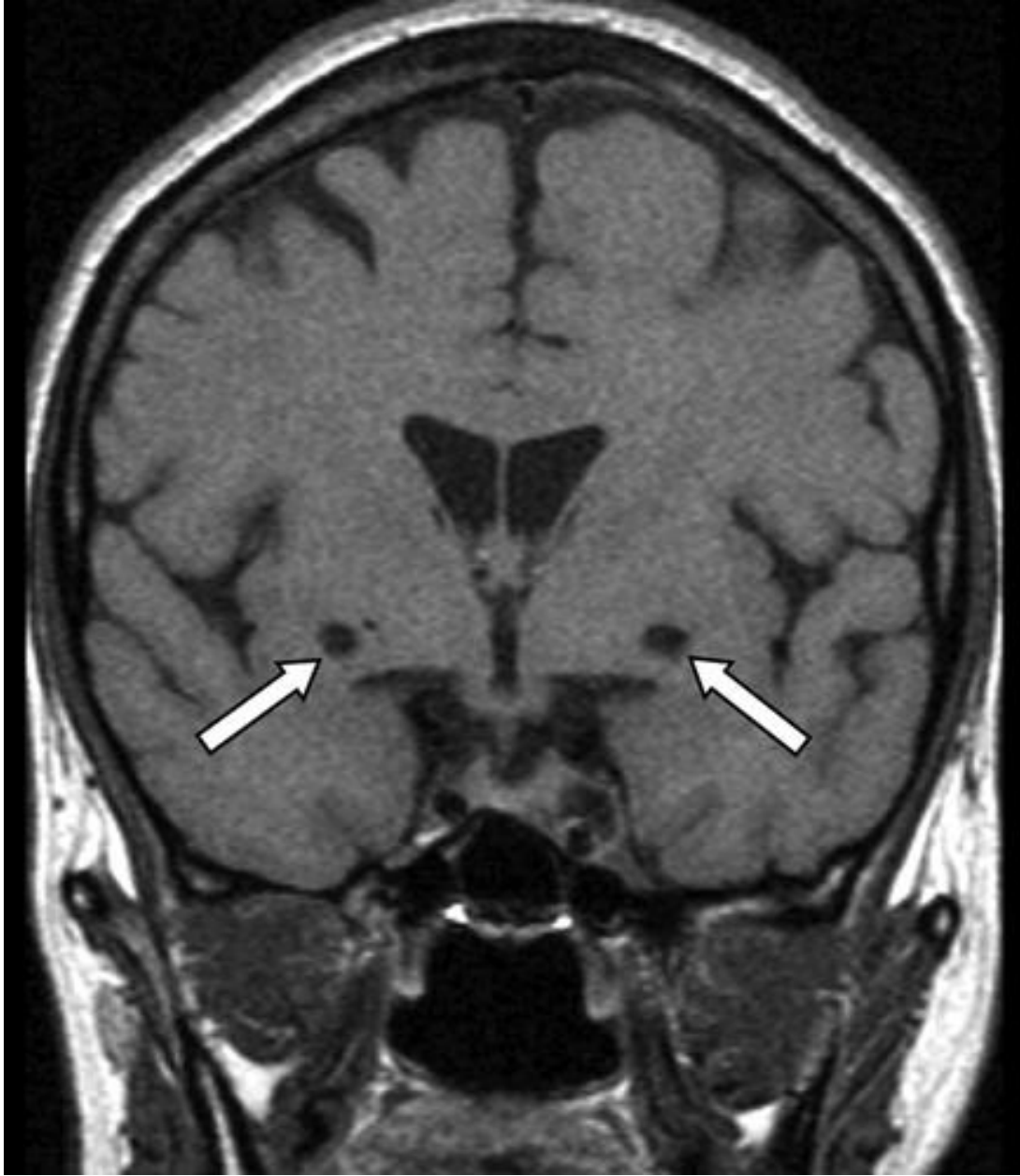


Figure 2: MR image showing Virchow Robin spaces (Qu et al., 2020).

1.2.3 Association between MRI features of Virchow-Robin spaces and CSVD

CSVD, a diverse collection of neuro-pathological changes with resultant clinical and neuroimaging findings, affects minute perforating arteries, arterioles, capillaries, as well as venules hence causing cerebral white matter and deep grey matter damage (Charidimou et al., 2016). CSVD is commonly associated with a proportional increase in age. The clinical presentation is largely determined by the resultant injury to the brain parenchymal tissue rather than the blood vessels involved. In this regard, CSVD encompasses brain injury involving parenchymal tissue residing in poorly collateralized subcortical areas and is associated with intracerebral vaso-occlusive and distal leptomeningeal pathologies (Mustapha et al., 2019).

Several etiopathogenic classifications, such as, genetically mediated cerebral autosomal dominant arteriopathy with subcortical ischemic strokes and leukoencephalopathy (CADASIL), venous collagenosis and immunologically mediated have been coined. However, the most predominant are amyloid and non-amyloid forms. Amyloid examples include hereditary and sporadic cerebral amyloid angiopathy (CAA), whereas non-amyloid include: age-linked as well as small vessel due to vascular risk factors as is the case in arteriolosclerosis (Pantoni, 2010). These are otherwise stratified into the following types: Type I associated with vasculogenic risk factors, Type II consisting of CAA and Type III encompassing all genetic or inherited subgroups with exception of CAA, the most common being CADASIL (Mestre et al., 2017).

CSVD is strongly associated with modifiable risk factors especially diabetes (DM) and hypertension (HTN), particularly in midlife (Debette et al., 2011; Power et al., 2017). Literature suggests a multifaceted nature-nurture balance underpinning the causation of CSVD. This balance involves a combination of genetic and vascular risk factors, particularly HTN, DM, smoking and alcohol intake. These factors increase the risk of developing CSVD. However, a combined effect

analysis of these risk factors accounts for a small fraction of the variance in CSVD imaging features; hence they may worsen the disease presentation rather than constitute the primary cause of CSVD (Brown et al., 2018c; Ihara & Yamamoto, 2016; Wardlaw, Smith, & Dichgans, 2013). Moreover, the mechanistic link between hypertension, diabetes, smoking, alcohol and CSVD is still poorly understood (Monteiro et al., 2021).

The pathogenesis of CSVD involves thickening of the respective arteriolar walls, hypoperfusion and subsequent development of white matter lesions. The involvement of Virchow-Robin spaces in the pathogenesis of CSVD, especially their enlargement, has proven quite useful as a key imaging diagnostic marker of neurovascular changes. Virchow-Robin spaces have since been regarded as early and reliable imaging characteristics in CSVD (Charidimou et al., 2016; Doubal et al., 2010). Virchow-Robin space pathologies related to CSVD such as endogenous A β aggregation are not well elucidated in literature (Mestre et al., 2017). The recent discovery of the glymphatic system, mainly constituted by Virchow-Robin spaces, offers a novel perspective on CSVD pathophysiology and the interplay between glymphatic failure and CSVD pathogenesis.

1.2.4 Predictive features of CVSD using MRI analysis of Virchow-Robin spaces

Neuroimaging remains the mainstay in the diagnosis of CSVD. This is due to the silent nature of the disease. Cerebral small vessel disease is often insidious in onset and is initially associated with mild clinical symptoms, both of which have rendered CSVD a frequently neglected neurovascular disease (Li et al., 2018). Some of the imaging findings in CSVD include white matter lesions, recent small subcortical infarcts, lacunes or lacunar infarcts, cerebral microbleeds and enlarged Virchow-Robin spaces. These pathological discoveries often present symptomatically as cognitive deterioration, amplified risk of stroke, as well as other neuropsychiatric disorders (Mestre et al., 2017).

In vivo detection of CSVD has continually remained to be inconsistent. Clinicians are often forced to count on imaging markers, predominantly a combination of perivascular white matter hyperintensities, microbleeds and lacunes which are late presentations of disease (Moran et al., 2012). The four-stage Fazekas scale has been widely used to visually quantify white matter hyperintensities in MRI data due to its reliability and ease of application. The scale spans from 0 to 3 with an increasing burden of periventricular white matter hyperintensities. A score of 0 indicates absence, 1 indicates the presence of caps/pencil-thin lining, 2 denotes smooth halo, and 3 designates irregular periventricular hyperintensities which extend far deep into the white matter. In the same breath, deep white matter hyperintensities (dWMH) are scored as 0 when absent, 1 when punctate foci are observed, 2 when there is commencement of confluence of foci, and 3 in cases where when significant confluent regions are seen.

Findings from the two subsets (periventricular and dWMH) of the scale are then computed to generate a total white matter hyperintensity burden score ranging from 0-6 with increasing severity (Fazekas et al., 1987; Kynast et al., 2018). A high Fazekas score, for instance in the presence of

confluent WMH, has been associated with significant cognitive deterioration as compared to lower scores such as in cases of punctate WMH. Clinically, the Fazekas scale has been instrumental in predicting cognitive performance in patients with Alzheimer's disease (Cedres et al., 2020).

The relationship between expanded Virchow-Robin spaces and CSVD has not been thoroughly investigated. Hitherto the above, regional differences and dimensions of Virchow-Robin spaces in MRI brain sections with CSVD compared to NCSVD are required. These analyses may be useful in the identification of diagnostic models and patterns that will serve as indices for early detection of Virchow-Robin space changes in patients with CSVD.

1.3 SIGNIFICANCE OF THE STUDY

CSVD remains the utmost predominant vascular source of dementia, a key player in mixed dementia, and the source of about 20% of all strokes globally (Norrving, 2008). Cerebral small vessel disease also worsens outcomes after strokes and is a principal source of disability, poor mobility and cognitive impairment (Brown et al., 2018). Currently, neuroimaging using magnetic resonance is gold standard in diagnosing CSVD. However, most features used occur late with symptomatology already set off in the patients. Understanding the consequences of CSVD and the morphology of Virchow-Robin spaces may help in identifying patterns that can be used as indicators for the early diagnosis of Virchow-Robin space or vascular-related changes in individuals with neurological diseases like CSVD. Additionally, the results can be helpful in creating a CSVD predictive diagnostic model.

1.4 STUDY JUSTIFICATION

Due to the increase in the ageing Kenyan population, coupled with an increase in life expectancy, morbidity and mortality resulting from CSVD are up trending (Akinyemi et al., 2019). CSVD is estimated to contribute to 10–20% of delayed dementia after stroke, 30–40% of vascular cognitive impairment and 2–3% of vascular dementia (Chawla et al., 2016). This heavy burden of morbidity and mortality is fast approaching estimates in other parts of the developed world. An understanding of the anatomy of Virchow-Robin spaces and the effects of CSVD may be useful in the identification of diagnostic models and patterns that will serve as indices for early detection of Virchow-Robin space or vascular-related changes in patients having neurological conditions such as CSVD.

1.5 CONCEPTUAL FRAMEWORK

The structure of cerebral blood vessels is affected by age, smoking, alcohol consumption, diabetes and hypertension. The resultant effect is vascular wall thickening which underpins the pathophysiology of CSVD. Diagnosis of CSVD is hinged on clinical evaluation and supporting imaging evidence of disease. The imaging markers relied upon in the diagnosis of CSVD, such as WMH, are late manifestations of disease. Virchow-Robin spaces, which form part of the glymphatic pathway, are described as early biomarkers of CSVD. As such, an in-depth characterization of Virchow-Robin spaces and their association with CSVD could offer a reliable approach for the early diagnosis of CSVD.

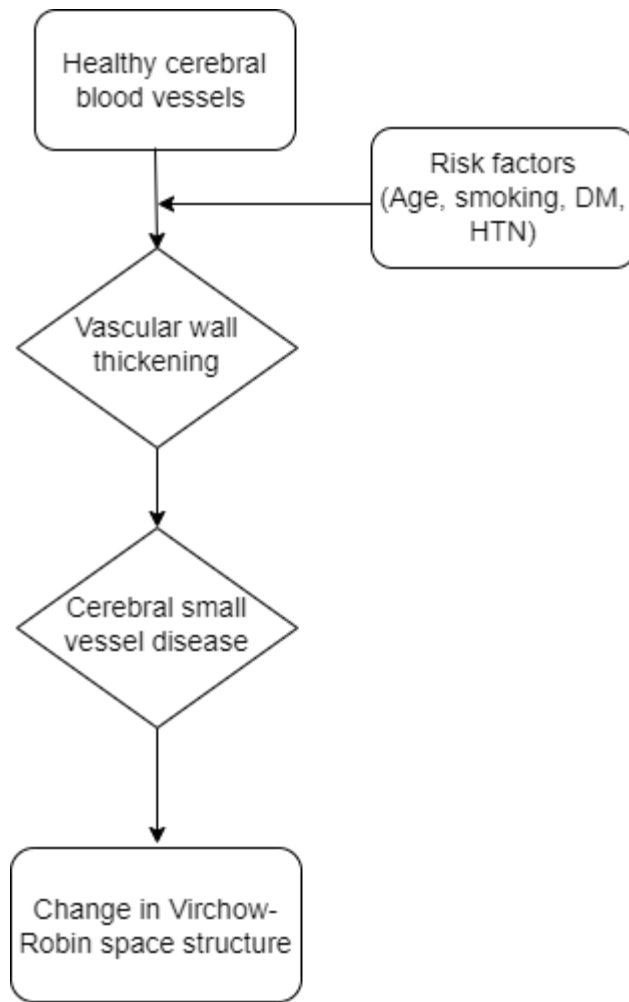


Figure 3 Conceptual Framework

1.6 STUDY QUESTION

What MRI features of Virchow-Robin spaces are associated with CSVD?

1.7 HYPOTHESIS

- **H₁:** There are MRI features of Virchow-Robin spaces associated with CSVD.

1.8 OBJECTIVES

1.8.1 Broad objective

To analyze the MRI features of Virchow-Robin spaces associated with CSVD.

1.8.2 Specific objectives

1. To describe MRI morphology and morphometry of Virchow-Robin spaces in CSVD and non-CSVD.
2. To determine the relationship between MRI features of Virchow-Robin spaces and CSVD.
3. To determine predictive diagnostic features of CSVD using MRI analysis of Virchow-Robin spaces.

CHAPTER TWO: MATERIALS AND METHODS

2.1 STUDY DESIGN

Analytical observational cross-sectional study

2.2 STUDY AREA AND SITE DESCRIPTION

Magnetic resonance images were obtained from the Kenyatta National Hospital (KNH) radiology department. The KNH imaging department serves as a regional referral centre with a nationally representative sample. Their imaging infrastructure includes a Philips MR Ingenia Elition 3.0T machine which produces high-resolution images. Strong magnetic fields and radio waves are combined in an MRI (Magnetic Resonance Imaging) scanner to produce precise images of the body's tissues. A patient's body aligns with the magnetic field produced by the device when they enter the MRI scanner. The body is then exposed to radio waves, which cause the hydrogen atoms in the tissues to emit weak signals. The receiver coils on the MRI scanner pick up these signals, and a computer then processes them to produce incredibly detailed images that doctors can view and examine. Organs, blood vessels, and abnormalities can all be seen thanks to the differentiation of body structures made possible by the diverse signals that different tissues emit. These high-quality images are widely used to study brain structure and function in development and disease (Alvarez-Linera, 2008). A review of records and data available at the department revealed that an average of 12 – 15 MRI scans of the brain are performed per day (360 to 450 MRI scans per month).

2.3 STUDY POPULATION

Data on demographics, alcohol consumption, cigarette smoking, clinical history (including symptoms, physical examination findings and medical comorbidities) and MRI scan features were collected from study subjects referred for MRI at the Kenyatta National Hospital radiology department. Study subjects recruited at the KNH radiology department included adults (> 18 years), of either sex (male or female) who granted their permission to participate in the study voluntarily.

2.3.1 Inclusion criteria

1. Patients above 18 years of age
2. Patients who had MRI scans of the brain taken.
3. Patients who gave informed consent to the study

2.3.2 Exclusion criteria

Study subjects with the following were excluded: any clinical contraindication to magnetic resonance imaging (Dill, 2008), Parkinson's disease, brain tumours, history of brain radiotherapy, hydrocephalus, trauma, syphilis, acquired immunodeficiency syndrome and epilepsy.

2.4 SAMPLE SIZE CALCULATION

[OpenEpi](#) version 3.01 updated 4th June 2013 was used to compute the number of MRI scans required for the study.

Sample size calculation for analytic cross-sectional studies (comparing two means):

N = Desired sample size

95% = Confidence interval (two-sided)

Alpha level of study (1.96 for an alpha level of 0.05)

80 % – Power

1 = Ratio of sample size (Group 2/Group 1)

The following means and standard errors of the means (13.5 (1.2) / 9.6 (1.4)) were obtained from Shen et al., (2021).

N= 54 per group.

Confidence Interval (2-sided)	95%		
Power	80%		
Ratio of sample size (Group 2/Group 1)	1		
	Group 1	Group 2	Difference*
Mean	13.5	9.6	3.9
Standard deviation	6.93	7.5	
Variance	48.0249	56.25	

Sample size of Group 1	54
Sample size of Group 2	54
Total sample size	108

*Difference between the means

2.5 SCREENING, RECRUITMENT, ENROLLMENT AND CONSENTING PROCEDURES

The lead researcher or a designated research assistant informed the patients who were sent to the KNH radiology department about the study. The trained research team screened participants who fulfilled the inclusion criteria and who provided informed consent, for symptoms before stratifying them into two groups based on the presence or absence of clinical symptoms suggestive of CSVD. Magnetic resonance scans were then obtained using the Philips Ingenia TM 3.0T system as per the protocol outlined in the section “Magnetic Resonance Imaging”.

Study subjects with clinical features and supporting MRI evidence of small vessel disease were included as the “CSVD” group. The “NCSVD” group included study subjects without any clinical features of CSVD. Their MRI scans were evaluated and reported as normal by the hospital radiologist and confirmed by the designated radiologist contracted by the principal investigator. Study subjects in these two groups were then matched for age and gender. Data including demographics, alcohol consumption, smoking and medical comorbidities were collected from the study subjects and their clinical charts using a questionnaire (attached in the appendix). From the participant MRI scans, absolute count of Virchow-Robin spaces, their length, width, area, anatomic location and presence of WMH – using Fazekas scale were recorded.

Coronavirus disease 2019 (COVID-19) guidelines from the ministry of health, as well as hospital guidelines, were followed throughout the collection of data. Study subjects’ privacy and confidentiality were observed.

2.6 VARIABLES

Dependent variables included length, width, anatomic location, count, and degree of WMHs using Fazekas scale.

Medical history variables included diabetes, medically diagnosed hypertension and social history of smoking (indicated in pack years), and alcohol consumption (units per week).

Independent variables: Age, Sex, Virchow-Robin space area

2.7 IMAGE ACQUISITION AND DATA COLLECTION PROCEDURES

Using the Philips Ingenia TM 3.0T system, structural brain MRI data were acquired using axial T1-weighted (T1w), axial T2-weighted (T2w), T2*-weighted (T2*w), and fluid-attenuated inversion recovery (FLAIR)-weighted whole-brain imaging sequences. Neuroimaging standards for research into CSVD were used to distinguish Virchow-Robin spaces from other lesions on MRI as well as their mimics (Wardlaw et al., 2011) {figure 4}.

	Recent small subcortical infarct	White matter hyperintensity	Lacune	Perivascular space	Cerebral microbleeds
Example image					
Schematic					
Usual diameter¹	≤ 20 mm	variable	3-15 mm	≤ 2 mm	≤ 10 mm
Comment	best identified on DWI	located in white matter	usually have hyperintense rim	usually linear without hyperintense rim	detected on GRE seq., round or ovoid, blooming
DWI	↑	↔	↔/(↓)	↔	↔
FLAIR	↑	↑	↓	↓	↔
T2	↑	↑	↑	↑	↔
T1	↓	↔/(↓)	↓	↓	↔
T2* / GRE	↔	↑	↔ (↓ if haemorrhage)	↔	↓↓

Figure 4: Findings on MRI for lesions related to CSVD (Wardlaw et al., 2011) Upper row: MRI scans and the lower row demonstrates a schematic representation of the MRI characteristics for changes related to CSVD, with a summary of imaging features in the lower row for individual lesions. DWI=diffusion-weighted imaging. FLAIR=fluid-attenuated inversion recovery. SWI=susceptibility-weighted imaging. GRE=gradient-recalled echo (Wardlaw et al., 2011).

In order to avoid classifying lacunes or WMH as Virchow-Robin spaces, the neuroradiologist assessed the Virchow-Robin spaces on T2w images by cross-checking against FLAIR and T1w (Potter et al., 2015). This grading determines the nearest classification on the scale ranging from 0 (no Virchow-Robin space), 1 (mild; 1-10 Virchow-Robin spaces), 2 (moderate; 11-20 Virchow-Robin spaces), 3 (frequent; 21-40 Virchow-Robin spaces) or 4 (severe; >40 Virchow-Robin spaces) based on the estimated number of Virchow-Robin spaces seen at the level of the centrum

semiovale (figure 2). Following an investigation of previous readily available rating scales, the Virchow-Robin spaces rating scale was created as a practical visual categorization tool for various healthy and sick populations across various ages. After that, it was examined and improved, and all information, including observer reliability, has been made public (Potter et al., 2015).

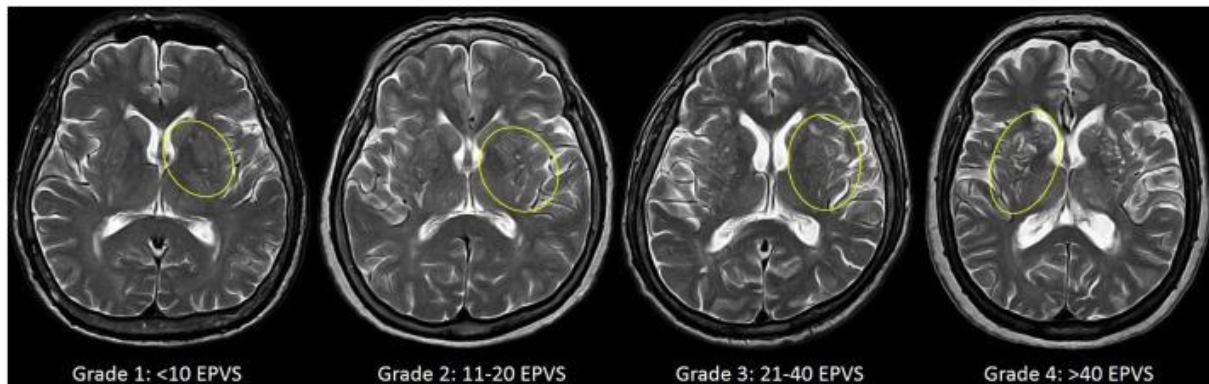


Figure 5: Visual rating of Virchow-Robin spaces as described by Potter et al., EPVS – Enlarged Virchow-Robin spaces (2015).

White matter hyperintensities (WMH) were examined and rated visually. This was done mainly on FLAIR, double-checking T1- and T2w as indicated. The four-stage Fazekas scale was used to visually quantify WMH on MRI scans. The scale spans from 0 to 3 with an increasing burden of periventricular white matter hyperintensities. A score of 0 indicates absence, 1 indicates the presence of caps/pencil-thin lining, 2 denotes smooth halo, and 3 designates irregular periventricular hyperintensities (PVH) which extend far deep into the white matter. Similarly, deep dWMH are scored as 0 when absent, 1 when punctate foci are observed, 2 when there is commencement of confluence of foci, and 3 in cases where large confluent areas are observed. Findings from the two subsets (PVH and dWMH) of the scale are then computed to generate a total white matter hyperintensity burden score ranging from 0-6 with increasing severity (Fazekas et al., 1987; Kynast et al., 2018) {figure 3}.

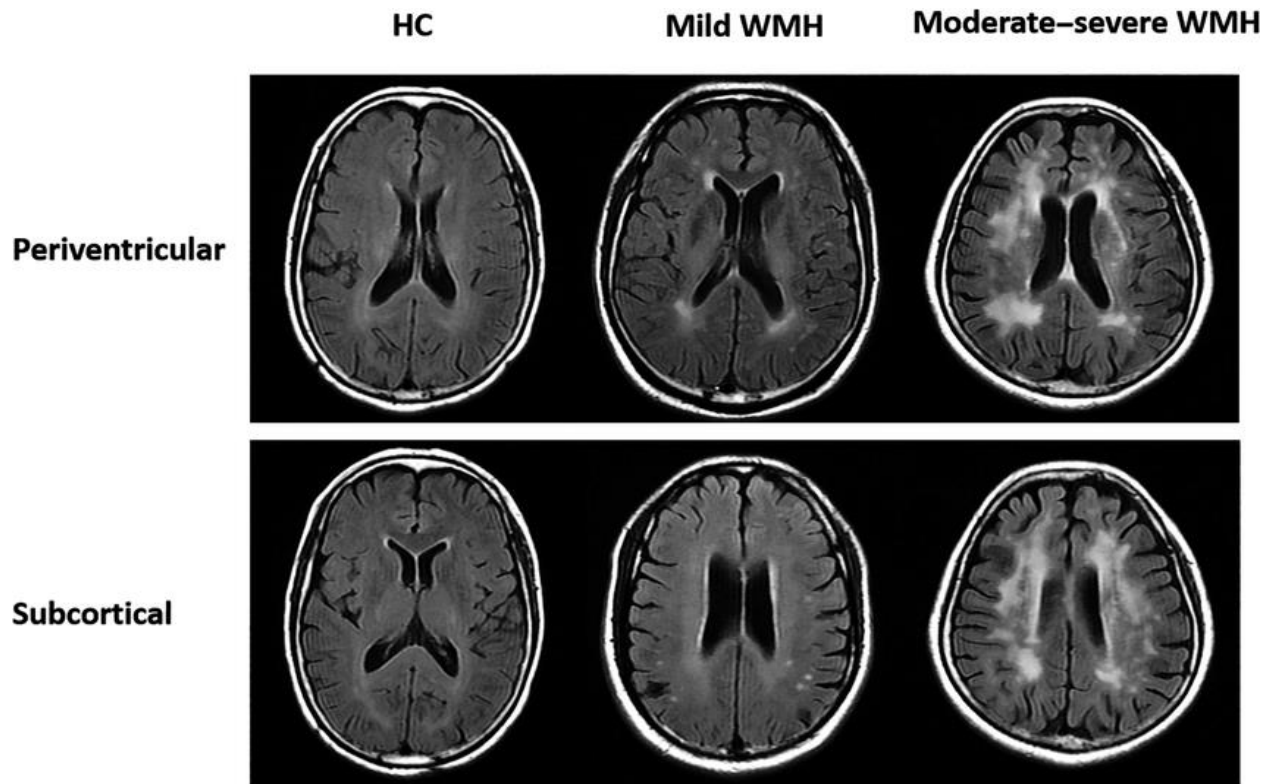


Figure 6: Grading of white matter hyperintensities using the Fazekas scale (Qu et al., 2020). HC – healthy controls with no white matter hyperintensities (WMH).

Connected component analysis, a function on MRI visualizing software used to detect connected regions in binary images, was used to measure individual Virchow-Robin space features such as diameter, length and area. The area was considered as the two-dimensional space covered by each Virchow-Robin space on the axial MRI. The length was considered to be the distance of the chief axis in the ellipsoid, the diameter was considered the 2nd longest axis, perpendicular to the ‘length’ (Ballerini et al., 2020) {figure 4}.

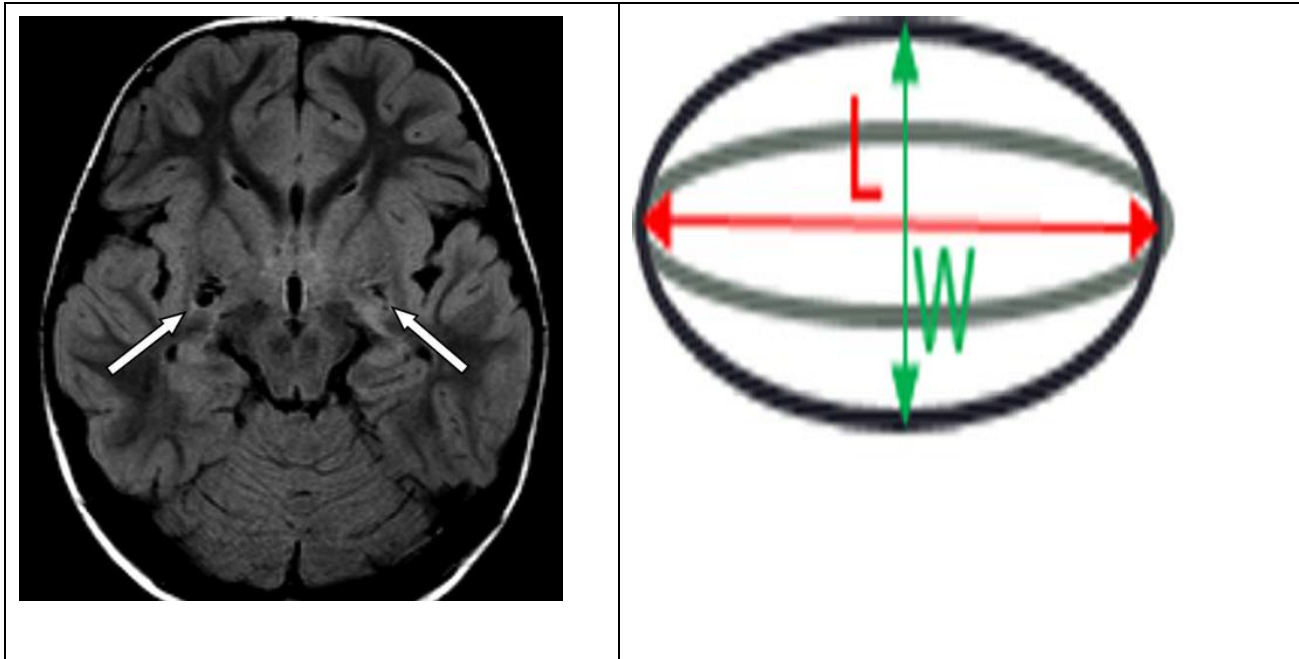


Figure 7: A schematic illustration of measurement of individual Virchow-Robin space to obtain the L –length, W – width or diameter and Virchow-Robin space area/size.

2.8 QUALITY ASSURANCE PROCEDURES

The examination of the MRI brain scan images used in the study and subsequent scoring was overseen by an independent radiologist. The data collection sheets, sample photographs as well as other entries were stored on a hard disk with a password restriction and backed up on email. SPSS version 25.0 (Chicago Illinois) analysis software was used for data cleaning (manual screening, analytical tests to check for invalid entries, duplicates, outliers and other inconsistencies).

2.9 ETHICAL CONSIDERATIONS

Ethical approval for this study was sought from the Kenyatta National Hospital- University of Nairobi Ethics and Research Committee (KNH-UON ERC) {Reference: P386/05/2021}. In addition, the study was registered at the KNH research department per institutional protocol. Serial numbers were used to code for patient names. Confidentiality was maintained throughout all stages of data collection and unauthorized persons did not have access to the data collected.

3.0 DATA ANALYSIS PLAN

Statistical tests were performed using SPSS version 28.0 (SPSS, Chicago, IL, U.S.A.) for Windows 10. Data normality was assessed using box plots and histograms. Depending on normality of the data set parametric or non-parametric tests was used in the comparison of age, substance use (number of alcohol units per week and number of pack-years), morphometric characteristics (Virchow-Robin space count, diameter, length and area) and total white matter hyperintensity burden score. The association between sex, comorbidities (diabetes and hypertension), cigarette and alcohol use, Potter's scale and Virchow-Robin space location was measured using crude and adjusted odd's ratio in multivariate and univariate logistic regression respectively. A *p-value* ≤ 0.05 was considered significant at a 95% CI.

CHAPTER THREE: RESULTS

3.1 DEMOGRAPHICS OF STUDY SUBJECTS

A total of 118 study subjects were included in this study. Of these, 43 (36 %) had cerebral small vessel disease (CSVD group), 75 study subjects, (64%) had no features of CSVD (NCSVD group). Study subjects in the CSVD group were older (55.1 ± 19.0 vs 44.9 ± 16.4 years, $p=0.003$), and were more likely to have hypertension (odds ratio, OR= 9.3, 95% CI 9.1-9.3, $p<0.001$) and diabetes (OR= 9.8, 95% CI 7.3-13.3, $p<0.001$). There were no differences found between the sexes ($p=0.588$), with alcohol use ($p=1.000$), or smoking ($p=0.228$) {Table 1}.

Table 1 : A comparative analysis of demographic, medical comorbidities and social characteristics of study subjects

Variable	CSVD (n=43; %)	NCSVD (n=75; 63.6%)	Total (n=118; 100%)	<i>p</i> -value*	
Age (Years) (Mean±SD)	55.1±19.0	44.9±16.4	49.4±18.2	0.003[†]	
Sex (Male)	27 (51.9%)	30 (45.5%)	57 (48.3%)	0.578 [#]	
Comorbidities	Hypertension	37 (71.2%)	14 (21.2%)	51 (43.2%)	<0.001[#]
	Diabetes	28 (53.8%)	7 (10.6%)	35 (29.7%)	<0.001[#]
Substance use	Alcohol use	30 (57.7%)	37 (56.1%)	67 (56.8%)	1.000 [#]
	No. of alcohol units per week	21.4±11.5	23.0±8.8	22.3±18.2	0.522 [†]
	Cigarette use	12 (23.1%)	9 (13.6%)	21 (17.8%)	0.228 [#]
	No. of pack-years	9.2±5.6	6.9±1.6	8.3±18.2	0.244 [†]

NB: *-the *p*-values are for CSVD-NCSVD comparison.

3.2 MRI MORPHOLOGY AND MORPHOMETRY OF VIRCHOW-ROBIN SPACES IN CSVD AND NCSVD

The number of Virchow-Robin spaces was observed to be significantly higher in the CSVD group (28.5±11.2 vs 12.2±8.5, p<0.001). Similarly, study subjects with CSVD had a significantly higher Potter's rating scale (p<0.001), a higher frequency of type 3 (p=0.007) Virchow-Robin space location, periventricular signal (p=0.005), deep white matter hyperintensities (p=0.001), total white matter hyperintensity burden score (p=0.001), wider (2.4±0.9 vs 1.7±0.7 mm, p<0.001), longer (2.4±0.8 vs 1.9±0.7 mm, p<0.001) and larger area (18.4±10.9 vs 11.5±6.5 mm², p<0.001) than NCSVD study subjects (Table 2, figure 5A-G).

Table 2: Difference in the morphology of PVS between CSVD and NCSVD groups

Variable	CSVD (43 subjects)	Study NCSVD (75 subjects)	p-value
No. of spaces (Mean±SD)	28.5±11.2	12.2±8.5	p<0.001[†]
Potter's scale (n, %)	None	0 (0%)	p<0.001[#]
	Mild	10 (19.2%)	
	Moderate	3 (5.8%)	
	Frequent	39 (75%)	
	Severe	0 (0%)	
Virchow-Robin space location (n, %)	Type 1	52 (100%)	p=0.119 [#]
	Type 2	20 (38.5%)	p=0.241 [#]
	Type 3	46 (88.5%)	p=0.007[#]
Periventricular signal (n, %)	Smooth halo	17 (32.7%)	p=0.005[#]
	Caps	24 (46.1%)	
	Irregular	4 (7.7%)	
Deep white matter hyperintensity (n, %)	Absent	7 (13.5%)	p=0.001[#]
	Beginning confluence	12 (23.1%)	
	Punctate foci	32 (61.5%)	
	Large confluent areas	2 (3.8%)	
	Absent	6 (11.5%)	22 (33.3%)
Total white matter hyperintensity burden score (Mean±SD)	2.5±1.3	1.6±1.1	p<0.001[†]
PVS diameter (mm, Mean±SD)	2.4±0.9	1.7±0.7	p<0.001[†]
PVS length (mm, Mean±SD)	2.4±0.8	1.9±0.7	p<0.001[†]
PVS area (mm², Mean±SD)	18.4±10.9	11.5±6.5	p<0.001[†]

Legend: Virchow-Robin space features in CSVD and NCSVD groups.

Figure 5A: Graph comparing the absolute count of Virchow-Robin spaces between CSVD and NCSVD groups.

Figure 5B: Graph comparing the number of study subjects (CSVD vs NCSVD) with periventricular white matter hyperintensities present on MRI versus the number of study subjects (CSVD vs NCSVD) without periventricular white matter hyperintensities i.e. absent on MRI.

Figure 5C: Graph comparing the number of study subjects (CSVD vs NCSVD) with deep white matter hyperintensities present on MRI versus the number of study subjects (CSVD vs NCSVD) without deep white matter hyperintensities i.e., absent on MRI.

Figure 5D: Graph comparing the total white matter hyperintensity burden score between CSVD and NCSVD groups.

Figure 5E: Graph comparing the mean diameter of Virchow-Robin spaces between CSVD and NCSVD groups.

Figure 5F: Graph comparing the mean length of Virchow-Robin spaces between CSVD and NCSVD groups.

Figure 5G: Graph comparing the mean area of Virchow-Robin spaces between CSVD and NCSVD groups.

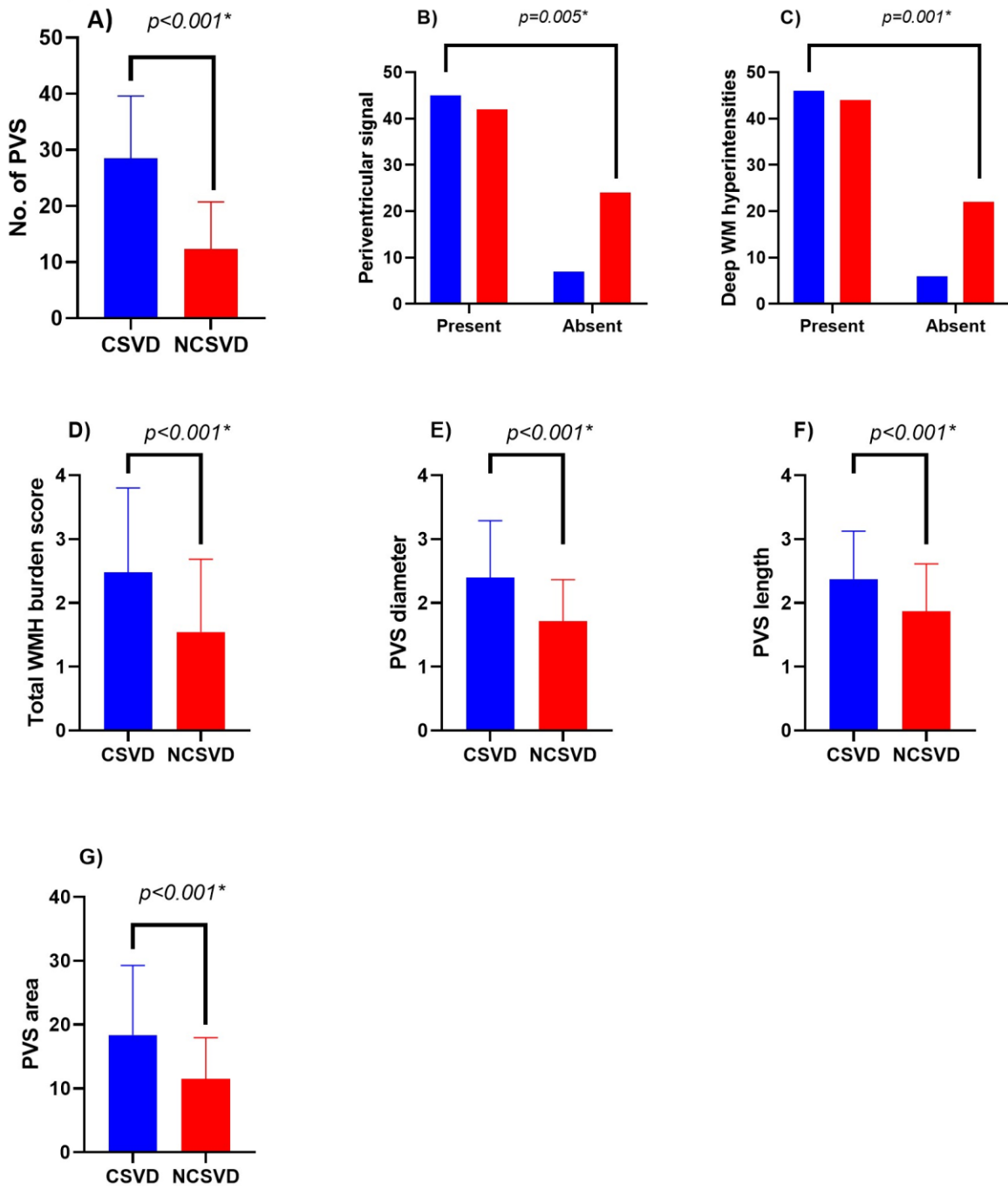


Figure 8 Graph comparing Virchow-Robin space features between CSVD and NCSVD groups.

*- Statistically significant; PVS- Virchow-Robin/periventricular space.

3.3 ASSOCIATION BETWEEN MRI FEATURES OF VIRCHOW-ROBIN SPACES AND CSVD

Univariate logistic regression analysis for demographic features, comorbidities, substance use and Virchow-Robin space features as predictors of CSVD revealed that increasing age (OR= 1.03, 95% CI 1.01-1.07), $p=0.003$), presence of hypertension (OR= 9.16, 95% CI 3.94-21.25, $p<0.001$) and diabetes (OR= 9.83, 95% CI 3.78-25.54, $p<0.001$), higher absolute number of Virchow-Robin spaces (OR= 1.17, 95% CI 1.11-1.23, $p<0.001$), type 3 (OR= 4.38, 95% CI 1.63-11.76, $p=0.003$) Virchow-Robin spaces location, presence periventricular signal (OR= 3.67, 95% CI 1.43-9.41, $p=0.007$), deep white matter hyperintensities (OR= 3.83, 95% CI 1.42-10.34, $p=0.008$), higher total white matter hyperintensity burden score (OR= 1.86, 95% CI 1.34-2.60, $p<0.001$), larger Virchow-Robin space diameter (OR= 3.03, 95% CI 1.84-5.93, $p<0.001$), length (OR= 2.66, 95% CI 1.47-4.82, $p=0.001$) and area (OR=1.13, 95% CI 1.06-1.20, $p<0.001$) were linked to higher chances of CSVD. However, only age (OR=1.05, 95% CI 1.00-1.09, $p=0.048$) was included in the multivariate adjusted logistic regression model, presence of diabetes (OR= 6.44, 95% CI 1.23-33.81, $p=0.028$) and absolute number of Virchow-Robin spaces (OR= 1.19, 95% CI 1.07-1.33, $p=0.001$) remained as significant predictors of CSVD (Table 3)

Table 3: Crude and adjusted odds ratio of factors predictive of CSVD.

Variable	Crude OR (95% CI)	Adjusted OR (95% CI)
Age	1.03 (1.01-1.07), <i>p</i> =0.003*	1.05 (1.00-1.09), <i>p</i> =0.048*
Sex	1.30 (0.63-2.68), <i>p</i> =0.485	1.88 (0.44-8.04), <i>p</i> =0.379
Hypertension	9.16 (3.94-21.25), <i>p</i> <0.001*	3.71 (0.53-25.91), <i>p</i> =0.187
Diabetes	9.83 (3.78-25.54), <i>p</i> <0.001*	6.44 (1.23-33.81), <i>p</i> =0.028*
Alcohol use	1.07 (0.51-2.23), <i>p</i> =0.859	2.51 (0.64-9.81), <i>p</i> =0.184
Smoking	1.90 (0.73-4.93), <i>p</i> =0.187	2.61 (0.66-10.35), <i>p</i> =0.170
Absolute number of PVS	1.17 (1.11-1.23), <i>p</i> <0.001*	1.19 (1.07-1.33), <i>p</i> =0.001*
Type 3 PVS location	4.38 (1.63-11.76), <i>p</i> =0.003*	1.85 (0.40-8.66), <i>p</i> =0.433
Periventricular signal	3.67 (1.43-9.41), <i>p</i> =0.007*	1.37 (0.22-8.51), <i>p</i> =0.736
Deep WMH	3.83 (1.42-10.34), <i>p</i> =0.008*	1.58 (0.26-9.70), <i>p</i> =0.619
Total WMH burden score	1.86 (1.34-2.60), <i>p</i> <0.001*	1.16 (0.52-2.62), <i>p</i> =0.714
PVS diameter	3.03 (1.84-5.93), <i>p</i> <0.001*	3.69 (0.32-42.44), <i>p</i> =0.294
PVS length	2.66 (1.47-4.82), <i>p</i> =0.001*	1.65 (0.19-14.25), <i>p</i> =0.651
PVS area	1.13 (1.06-1.20), <i>p</i> <0.001*	1.10 (0.84-1.44), <i>p</i> =0.476

PVS- Virchow-Robin/ periventricular space; WMH- white matter hyperintensities, OR- odds ratio

3.4 PREDICTIVE FEATURES OF CSVD USING MRI ANALYSIS OF VIRCHOW-ROBIN SPACES

Receiver operating curves (ROC) were generated for quantitative features of Virchow-Robin spaces for predicting CSVD. The number of Virchow-Robin gaps had an area under the curve (AUC) of 0.87 (95% CI 0.80–0.94; *p*<0.001). A cutoff of 19.5 Virchow-Robin spaces was discovered by analysis of ROC data to be related with 0.81 sensitivity and 0.82 specificity, respectively (Figure 6A). The Virchow-Robin space length AUC was 0.69 (95% CI 0.60-0.79; *p*=0.003), with 0.67 sensitivity and 0.61 specificity at a threshold of 2.03 mm (Figure 6B). AUC for Virchow-Robin space diameter was 0.71 (95% CI 0.62-0.81; *p*<0.001), with 0.67 sensitivity and 0.65 specificity at a threshold of 1.90 mm (Figure 6C). A 1.5 cutoff showed 0.81 sensitivity and 0.48 specificity, and the AUC for the overall white matter hyperintensity burden score was 0.69 (95% CI 0.60-0.79; *p*<0.001) (Figure 6D). Similarly, the AUC for total white matter hyperintensity burden score was 0.74 (95% CI 0.65-0.84; *p*<0.001), with a $\geq 12.5\text{mm}^2$ cutoff displaying 0.75 sensitivity and 0.67 specificity (Figure 6E).

Legend: ROC curves of quantitative features of Virchow-Robin spaces for predicting CSVD.

Figure 9A: ROC curve of the absolute number of Virchow-Robin spaces for predicting CSVD.

Figure 9B: ROC curve of the Virchow-Robin space length for predicting CSVD.

Figure 9C: ROC curve of the Virchow-Robin space diameter for predicting CSVD.

Figure 9D: ROC curve of the total white matter hyperintensity burden score for predicting CSVD.

Figure 9E: ROC curve of the Virchow-Robin space area for predicting CSVD.

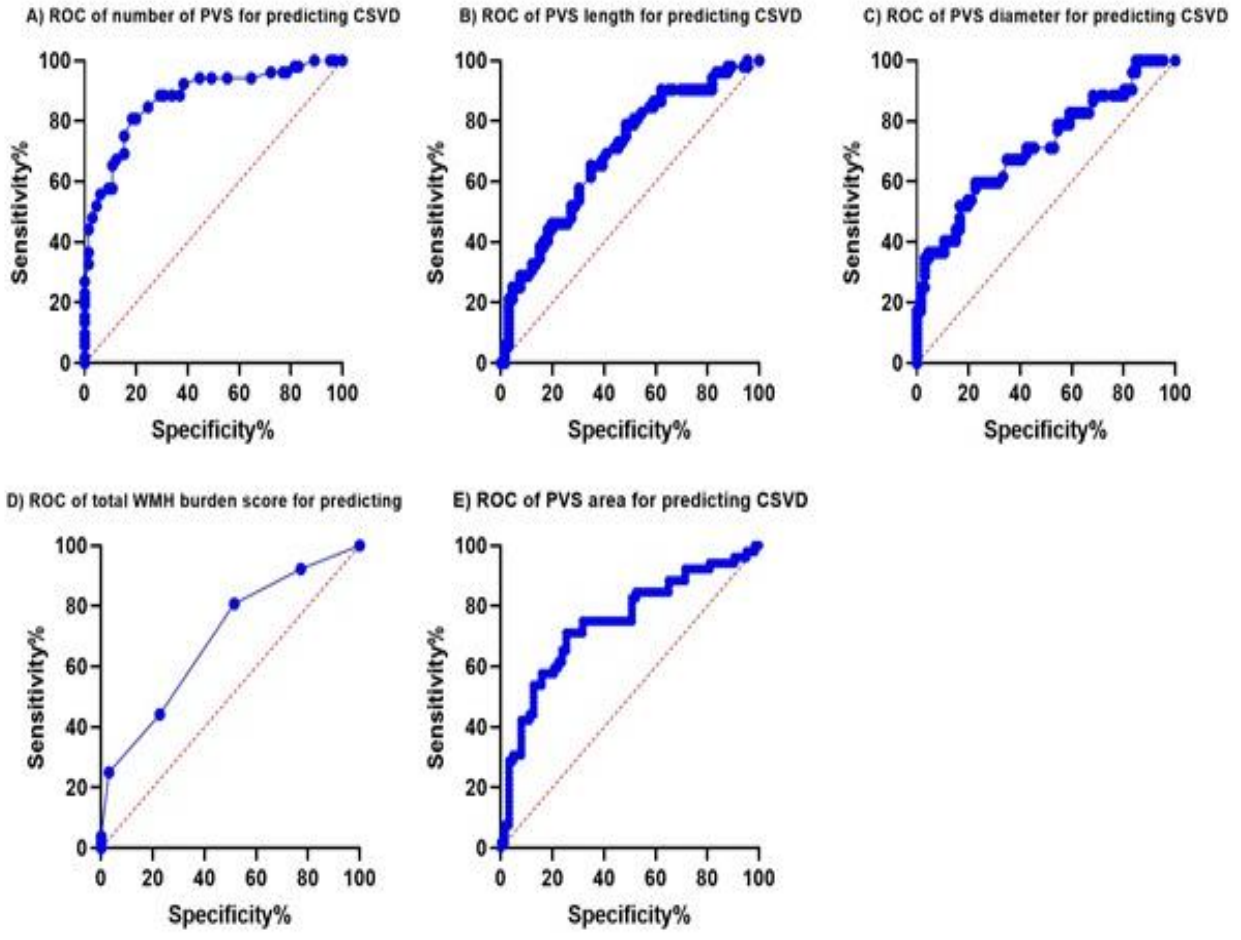


Figure 9 ROC curves of quantitative features of Virchow-Robin spaces for predicting CSVD

CHAPTER FOUR: DISCUSSION AND CONCLUSION

The findings of the current study demonstrated a relationship between the MRI morphology and morphometry of Virchow-Robin spaces and CSVD. It was also demonstrated that there was a strong link between age, diabetes, and the total number of Virchow-Robin gaps. The absolute number of Virchow-Robin spaces showed the highest sensitivity and specificity for the detection of CSVD on MRI.

4.1 DEMOGRAPHIC, COMORBIDITIES AND SOCIAL CHARACTERISTICS

Cerebral small vessel disease is thought to be caused by a multifaceted nature-nurture balance involving genetic and vascular risk factors. These factors appear to increase the risk of CSVD. (Brown et al., 2018; Ihara & Yamamoto, 2016; Wardlaw et al., 2013). In the current study, study subjects with imaging and clinical evidence of CSVD were significantly older, and more likely to have HTN and DM. Alcohol use, smoking and sex differences did not have a significant effect on the likelihood of having CSVD. These points were highlighted in table 1.

An increase in age is linked to a higher probability of developing CSVD. As such, age is termed the greatest, irreversible risk factor for cerebral vascular disease (Cuadrado-Godia et al., 2018; De Silva & Faraci, 2020). It is worth noting, however, that the mean age of study subjects diagnosed with CSVD herein (55 years) is younger than that reported by other workers in studies evaluating predictors for CSVD including age (59 -79 years) (Backhouse et al., 2021; van Dijk et al., 2008). Worldwide, CSVD affects approximately 5% of people over the age of 50 years and nearly every person >90 years (Cannistraro et al., 2019). Conversely, cohorts who had accelerated/ early development of CSVD, with a mean age of 49 years, have been described by Arntz et al., (2016). Early development of CSVD is attributed to the occurrence of strokes, ischemic and transient ischemic attacks (TIA) in childhood which leads to accelerated cerebral ageing, by 10 – 20 years,

and increased vulnerability to vascular risk factors (Arntz et al., 2016). The justification for the detection of CSVD in a relatively younger sample population remains elusive. Large population-based studies conducted in the region may provide further insight.

CSVD is also linked to modifiable risk factors especially HTN and DM, particularly in the fifth decade of life (Debette et al., 2011; Power et al., 2017). In the current study, the odds of having CSVD were significantly higher, on average nine-fold, in the study subjects who were diagnosed to have hypertension or diabetes (as per table 1). Abraham et al., (2016) and Liu et al., (2018) have reported similar findings with approximately an eight-fold increase. However, the mechanistic link between hypertension, diabetes and CSVD and how these comorbidities contribute to the evolution of the disease is still poorly understood (Monteiro et al., 2021). Several theories have been posited to explain the cerebrovascular dysfunction associated with these comorbidities (hypertension and diabetes). Chronic vascular changes caused by diabetes include macrovascular disorders for instance cardiovascular and cerebrovascular large vessel disease as well as nephropathy, retinopathy and neuropathy as well, which are microvascular disorders (Chawla et al., 2016). The buildup of glycated by-products in type II diabetes causes inelasticity of the small arteries (Brundel et al., 2014). Diabetes-associated dysautonomia leads to cerebrovascular dynamics dysfunction which could also lead to CSVD (Azevedo et al., 2011).

Blood vessel remodelling, increased cerebro-vascular resistance, hypoperfusion of the cerebrum and diminished neurovascular coupling (NVC) are distinct phenomena in hypertensive disease. The vasoactive signals released as a result of local increases in neuronal activity cause strong vascular responses to accompany the dynamic process of neurovascular coupling. Functional hyperemic responses are based on defective NVC processes. Increases in neuronal activity cause rapid blood flow redirection providing uninterrupted blood supply which is crucial for brain

viability as well as ongoing brain activities (Hosford & Gourine, 2019; Iadecola, 2017). The molecular interactions that determine brain perfusion occur at the lowest level at the neurovascular unit (NVU). It is made up of neurons, vascular smooth muscle cells, astrocytes, and endothelial cells (Iadecola, 2017). The dynamic communication between these elements, as well as the provision of energy substrates and the removal of waste metabolites for neurons, all contribute to the moment-to-moment control of arteriole and capillary blood flow (Presa et al., 2020). In addition, arteries undergo various remodeling processes as a result of increased intravascular pressure, including hypertrophic remodeling, hypotrophic remodeling, inward remodeling, and arterial stiffening (Presa et al., 2020; Renna et al., 2013).

Due to the link between heavy alcohol intake and vascular risk factors inclusive of high blood pressure, atrial fibrillation, haemorrhagic stroke, and heart failure, excessive drinking is indirectly linked to vascular dementia (Schwarzinger et al., 2018). Alcohol use in the current study was 21 and 23 units per week for the CSVD and non-CSVD groups, respectively, with no discernible difference in terms of units, on average (as per table 1). The rationale for an association between increased alcohol intake and CSVD is similar to what is observed in smoking, as discussed below.

Smoking has been linked to a two-fold surge in the risk of Alzheimer's disease and dementia (Gons et al., 2011). The exact process is unknown, although CSVD could play a role since it is linked to both the risk factor (smoking) and the consequence (death) (Gons et al., 2011; Román et al., 2002). The current study demonstrates a higher percentage of smokers in the CSVD group (23% vs 13%), though the difference was not statistically significant. Similar findings, a higher proportion of smokers with features of CSVD, have been reported by other workers in various populations (Asian, including Japanese and Caucasians). However, the differences observed did not meet statistical significance (as per table 1) (Hara et al., 2019; Staals et al., 2014; Wardlaw et al., 2013;

van Dijk et al., 2008). Smoking as a modifiable risk factor has been reported to have a synergistic effect with CSVD when combined with other modifiable risk factors inclusive of HTN (Hara et al., 2019). As such, concerted efforts for managing HTN, smoking, and diabetes may be key in preventing CSVD.

4.2 MRI MORPHOLOGY AND MORPHOMETRY OF VIRCHOW-ROBIN SPACES IN CSVD AND NCSVD

Virchow-Robin spaces are frequently visualized since the introduction of high-resolution MRI. (Groeschel et al., 2006; Oztürk & Aydingöz, 2002). In the current study, all study subjects recruited had one or more Virchow-Robin spaces visualized. In addition to typical CSVD characteristics, Wardlaw et al. (2013) also found an increase in the number of Virchow-Robin spaces on MRI with aging, based on visual scores.

The average number of Virchow-Robin spaces visualized herein, on T2 – weighted and FLAIR sequences, at the basal ganglia level, were found to be more than double in the CSVD group compared to the NCSVD group (figure 5A). The absolute count of Virchow-Robin spaces reported differs from those by other workers (Ballerini, Booth, Valdés Hernández, et al., 2020). Ballerini et al., (2020) pioneered an analytical method comparing multiple measures of Virchow-Robin space enlargement derived using a computational segmentation method. Their findings revealed that each MRI scan had on average 258 total Virchow-Robin spaces visible (23 – 536) as compared to an average of 28 (17 – 39) spaces reported in the current study. This reveals a marked difference. In contrast to the current study, which comprised younger study participants (Mean age 55 years), the cohort recruited in the study by Ballerini et al. (2020) was chosen from a sample of a Scottish cohort of community-dwelling persons starting of their 8th decade. In addition, the computation segmentation method employed the use of automated tools that accounted for all Virchow-Robin

spaces in the MRI obtained as opposed to the current study that relied on manual counting at the basal ganglia level.

Despite the difference noted in the absolute count, the use of the qualitative visual rating scores developed by Potter et al., (2015) yielded similar results. Following a review of existing published rating scores, the Virchow-Robin space rating scale was created as a practical visual categorization tool in a few healthy and unwell populations across a range of ages. These ordinal scales are trustworthy, especially when computational segmentation methods are not widely available, despite the fact that they are essentially insensitive due to a lack of categories, floor and ceiling effects, and a vulnerability to observer bias (Aribisala et al., 2014).

The association between the location of Virchow-Robin spaces and a diagnosis of CSVD on MRI brain images has hitherto not been described in literature. The inconsistency seen in anatomic location and the connection with other biomarkers of CVSD reveal a difference in the pathophysiology of proximal vs distal small Virchow-Robin spaces (Mitchell, 2009). High pulsatility is harmful to low-resistance organs including the brain (Kalvach et al., 2007). The lenticulostriate probing branches of the middle cerebral arteries, which correspond to type I Virchow-Robin gaps, supply the substantia innominata and basal ganglia. The perforating branches are initially encountered as the pulse-wave reaches the brain. These smaller channels are more susceptible to systemic hemodynamic stressors because of the sudden shift in size from wide to penetrating arteries, which may explain why small Virchow-Robin gaps at these proximal sites more accurately forecast vascular outcomes (Cole & Yates, 1968).

Study subjects in the Northern Manhattan Study with Virchow-Robin spaces in the posterior fossa had a 26% greater risk of myocardial infarction (MI) per Virchow-Robin space observed, whereas those with evidence of subcortical Virchow-Robin spaces had only a 1% increased risk of MI

(Gutierrez et al., 2017). While type I and type II basal ganglia PVSs are more common in vascular dementias and hypertension, type III subcortical Virchow-Robin spaces are more common in nonvascular dementias and multiple sclerosis (Etemadifar et al., 2011; Zhu et al., 2010). Another plausible rationale for the disparities in the rates of Virchow-Robin spaces according to location may be associated with the related anatomical arrangement of the meninges that encase penetrating arteries. Lenticulostriate arteries, corresponding to type I Virchow-Robin spaces, have a double meningeal wrapping compared to the perforating medullary arteries corresponding to type II Virchow-Robin spaces, with a single-layered coating (Pollock et al., 1997). Although it is still unknown if glymphatic drainage varies depending on anatomic location, the structural configuration of the meningeal layers may influence how well interstitial fluids are drained between the two locations.

4.3 ASSOCIATION BETWEEN MRI FEATURES OF VIRCHOW-ROBIN SPACES AND CSVD

The interplay between Virchow-Robin spaces and disease states was first discussed by Durant-Fardel in the 1800s when he described dilated Virchow-Robin spaces in pathological states (Durant-Fardel., 1843). With the advent of MRI technology, the capacity to study Virchow-Robin spaces, in vitro, has even further provided increasing evidence of this association (Kwee and Kwee, 2007). Enlarged Virchow-Robin spaces have been shown to correlate with elevated risk of stroke, vascular dementia, systemic inflammation, multiple sclerosis, reduced cognitive function, hypertension, and reduced vessel elasticity associated with low Von-Willebrand factor levels (Brown et al., 2018). Morphological and morphometric alterations in Virchow-Robin spaces have been observed in CSVD, with adjuvant pathological alterations in brain tissue such as white matter hyperintensities. The STRIVE guidelines define Virchow-Robin spaces as key features in aiding the description of pathological features in CSVD (Wardlaw et al., 2013).

After accounting for potential confounders, in the multivariate-adjusted logistic regression model, only the absolute number of Virchow-Robin spaces among the PVS morphometric was found to be a significant predictor of CSVD displaying odds of 1.19 (as per table 3). Hence, Virchow-Robin space counts shows potential for their use as diagnostic markers in CSVD as part of the continuum in MRI features. The significant increase in Virchow-Robin space numbers in CSVD could be attributed to the compensatory angiogenesis which occurs in pathological states involving loss of blood vessels to allow for vasculature structural adaptation. The angiogenesis propagates the consequences of CSVD and hence attempts to promote tissue repair and restore the functional supply of oxygen and nutrients necessary for tissue regeneration. This also provides a scaffold for the intravasation of neural progenitor cells towards the cerebral parenchymal lesions (Jiang et al., 2021).

Rudie et al., (2018) have reported Virchow-Robin spaces with an average size of < 2 mm in cross-sectional diameter. When dilated Virchow-Robin spaces exhibit sizes >5 mm and giant Virchow-Robin spaces can expand and enlarge up to >1.5 cm in size. The current study observed an average of 2.4 ± 0.9 mm in CSVD study subjects and 1.7 ± 0.7 mm in non CSVD study subjects (figure 5E). This is in keeping with previous literature and though the dilated variant is mostly observed in CSVD as well as in some cases (1.6% to 3%) of healthy individuals, especially with advancing age, our findings demonstrated an interval measurement between normal and dilated diameters in CSVD cases. The modified description of CSVD pathological features in the STRIVE guidelines defines Virchow-Robin spaces as having a diameter of <3 mm when imaged perpendicular to the vessel course. This definition further raises awareness of the possibility that some Virchow-Robin spaces may have diameters smaller than 3 mm and acknowledges an overlap between larger Virchow-Robin spaces and small lacunes (Brown et al., 2018; Wardlaw et al., 2013).

Virchow-Robin spaces form a crucial structural component in normal brain homeostasis. Their alterations, particularly in dilated, are associated with CSVD. While the cause-effect mechanisms surrounding dilated Virchow-Robin spaces in CSVD remain unclear, several theories such as systemic inflammation have been proposed (Brown et al., 2018). The main rationale for dilation of Virchow-Robin spaces in CSVD is the associated systemic inflammatory processes that occur, leading to attendant Virchow-Robin space dysfunction and consequently WMH. While the role and triggers for the inflammation remain partially elucidated, excessive salt intake and underlying inflammatory conditions, which increase the burden of CSVD, have been attributed (Aribisala et al., 2014; Wiseman et al., 2016). Elevated pro-inflammatory markers tend to cause accumulation of inflammatory cells around Virchow-Robin spaces which lead to the destruction of the extracellular matrix with associated loss of blood-brain barrier (BBB) integrity, along with prompting demyelination. As a result of the aggregation of inflammatory cells within the Virchow-Robin spaces, blood vessel remodeling occurs leading to reduced blood flow, alterations in fluid clearance, hypoperfusion and hypoxia, the key mechanisms in CSVD pathophysiology (Martinez Sosa and Smith, 2017).

The reduced fluid clearance in this context stems from the loss of pulsatility and vessel stiffness of cerebral arterioles. The resulting hypoxia and neuronal apoptosis, trigger activation of macrophages and microglia which worsen BBB dysfunction and further enlarge Virchow-Robin spaces. Reduced cerebral blood flow and vascular dysfunction, therefore, remain key in the pathogenesis of CSVD. However, their temporal association and relationship with distended Virchow-Robin spaces are not well understood (Brown et al., 2018). The effects of systemic inflammation may however explain the observed increased diameter, length and area observed in the present study.

4.4 PREDICTIVE FEATURES OF CSVD USING MRI ANALYSIS OF VIRCHOW-ROBIN SPACES

Due to the challenges in visualizing small vessel damage in vivo, brain parenchymal changes caused by CSVD, inferred from MRI findings such as lacunar infarcts, WMH, and deep haemorrhage have formed hallmarks of the disease and hence for a long time, CSVD has been directly equated to cerebral parenchymal lesions. Over time, the definition of CSVD has grown to include the pre-ischemic events that occur in the setting of vascular damage and endothelial dysfunction (Bolanzadeh et al., 2012). This extended view of CSVD has hence provided platforms for possible interventions targeted towards arresting CSVD progression before the occurrence of irreparable brain damage. Virchow-Robin spaces and their close association with cerebral blood vessels have rendered their utility paramount in the early detection and diagnosis of CSVD.

Findings from the present study observed the number of Virchow-Robin spaces as the strongest predictor of CSVD with an area under the curve of 0.87 with a 0.81 sensitivity and 0.82 specificity, while the length demonstrated the weakest prediction (AUC: 0.69, 0.67 sensitivity and 0.61 specificity) among the quantitative features observed in CSVD cases (as per figure 9A). Though weakest compared to the other Virchow-Robin space morphometric indices, length was found to have almost similar predicting power to WMH, both having an AUC of 0.69 despite the slightly higher sensitivity observed in WMH. Virchow-Robin space morphometric features the absolute number of Virchow-Robin spaces, seem to offer great potential as an adjunct predictor in the early diagnosis of CSVD (as per figure 9B and 9D). Furthermore, among the Virchow-Robin space morphometric features, only the absolute count was found to be a significant predictor of CSVD in multivariate-adjusted logistic regression models (as per figure 9A).

CONCLUSION

The morphology and morphometry of Virchow Robin spaces, from our study, has been shown to be affected by CSVD. Study subjects with CSVD have been seen to have a dilated Virchow Robin spaces and an increased number of type I and II VRS. MRI features of VRS associated with CSVD include: a high Potter's scale, a high frequency of type III Virchow-Robin spaces, larger Virchow-robin spaces and a high absolute count of Virchow-robin spaces. The absolute number of Virchow-Robin spaces provided the best prediction model for CSVD, with the highest sensitivity and specificity, in comparison to the routinely used total white matter hyperintensity burden score. Consequently, there are MRI features of VRS that are associated with CSVD that can be used as an early diagnostic marker for CSVD.

RECOMMENDATIONS :

Further research with a larger sample size to investigate whether incorporation of the absolute count of Virchow-Robin spaces, with a preliminary cut off of ≥ 19.5 , can be considered to aid in the early detection and diagnosis of CSVD in vivo. In addition to this, we recommend the incorporation of analyzing MRI features of VRS in the diagnosis of CVSD.

SUGGESTIONS FOR FURTHER STUDIES :

1. Conduct large population-based studies. These will provide representative data on uncommon phenomena relating to CVSD such as early-onset disease in the younger population.
2. The use of computational segmentation methods for image analysis. Machine learning and artificial intelligence would provide an accurate and reproducible analysis of MRI scans. The data obtained would also be comparable to that collected in other parts of the world using similar standardized methods.

STUDY LIMITATIONS AND DELIMITATIONS

STUDY LIMITATIONS

1. Intra-observer errors acquired during measurement of study parameters.
2. Inter-observer errors acquired during measurement of study parameters.

STUDY DELIMITATIONS

1. Each variable was assessed and/or measured twice to reduce intra-observer error.
 2. Each variable was assessed and/or measured by two investigators to reduce inter-observer error.
- Any arising disparities were settled through a consensus and when need be, a third investigator.

REFERENCES

1. Abraham, H. M., Wolfson, L., Moscufo, N., et al., (2016). Cardiovascular risk factors and small vessel disease of the brain: Blood pressure, white matter lesions, and functional decline in older persons. *J Cereb Blood Flow Metab*, 36(1), :. 132–142.
2. Achariyar, T. M., Li, B., Peng, W., et al., (2016). Glymphatic distribution of CSF-derived apoE into brain is isoform specific and suppressed during sleep deprivation. *Mol Neurodegener* 11(1), p. 74.
3. Akinyemi, R. O., Owolabi, M. O., Ihara, M., et al., (2019). Stroke, cerebrovascular diseases and vascular cognitive impairment in Africa. *Brain Res Bull* (145), :. 97–108.
4. Alosco, M. L., Gunstad, J., Xu, X., et al., (2014). The impact of hypertension on cerebral perfusion and cortical thickness in older adults. *J Am Soc Hypertens*, 8(8), :. 561–570.
5. Alvarez-Linera, J. (2008). 3T MRI: advances in brain imaging. *Eur J Radiol*, 67(3), :. 415–426.
6. Aribisala, B. S., Wiseman, S., Morris, Z., et al., (2014). Circulating inflammatory markers are associated with magnetic resonance imaging-visible perivascular spaces but not directly with white matter hyperintensities. *Stroke*, 45(2), :. 605–607.
7. Arntz, R. M., van den Broek, S. M., van Uden, I. W., et al., (2016). Accelerated development of cerebral small vessel disease in young stroke patients. *Neurology*, 87(12), :. 1212–1219.
8. Azevedo, E., Castro, P., Santos, R., (2011). Autonomic dysfunction affects cerebral neurovascular coupling. In *Clin Auton Res*, 21(6), :. 395–403.
9. Backhouse, E. V., Shenkin, S. D., McIntosh, A. M., et al., (2021). Early life predictors of late life cerebral small vessel disease in four prospective cohort studies. *Brain*, 144(12), : 3769–3778.

10. Ballerini, L., Booth, T., Valdés Hernández, M. D. C., et al., (2020). Computational quantification of brain perivascular space morphologies: Associations with vascular risk factors and white matter hyperintensities. A study in the Lothian Birth Cohort 1936. *Neuroimage Clin*, 25, p. 102120.
11. Braffman, B. H., Zimmerman, R. A., Trojanowski, J. Q., et al., (1988). Brain MR: pathologic correlation with gross and histopathology. 1. Lacunar infarction and Virchow-Robin spaces. *AJR Am J Roentgenol*, 151(3), :. 551–558.
12. Brown, R., Benveniste, H., Black, S. E., et al., (2018). Understanding the role of the perivascular space in cerebral small vessel disease. *Cardiovasc. Res.*, 114(11), :. 1462–1473.
13. Brundel, M., Kappelle, L. J., & Biessels, G. J. (2014). Brain imaging in type 2 diabetes. *Eur Neuropsychopharmacol*, 24(12), :. 1967–1981.
14. Cannistraro, R. J., Badi, M., Eidelman, B. H., et al., (2019). CNS small vessel disease: A clinical review. *Neurology*, 92(24), :. 1146–1156.
15. Cedres, N., Ferreira, D., Machado, A., et al., (2020). Predicting Fazekas scores from automatic segmentations of white matter signal abnormalities. *Aging*, 12(1), 894–901.
16. Charidimou, A., Pantoni, L., & Love, S., et al., (2016). The concept of sporadic cerebral small vessel disease: A road map on key definitions and current concepts. *Int J Stroke*, 11(1), :. 6–18.
17. Chawla, A., Chawla, R., & Jaggi, S., et al., (2016). Microvascular and macrovascular complications in diabetes mellitus: Distinct or continuum? *Indian J Endocrinol Metab*, 20(4), :. 546–551.
18. Cole, F. M., & Yates, P. O. (1968). Comparative incidence of cerebrovascular lesions in normotensive and hypertensive patients. *Neurology*, 18(3), :. 255–259.

19. Cuadrado-Godia, E., Dwivedi, P., Sharma, S., et al., (2018). Cerebral Small Vessel Disease: A Review Focusing on Pathophysiology, Biomarkers, and Machine Learning Strategies. *J Stroke*, 20(3), .: 302–320.
20. De Silva, T. M., & Faraci, F. M. (2020). Contributions of Aging to Cerebral Small Vessel Disease. *Annu Rev Physiol*, 82, .: 275–295.
21. Debette, S., Seshadri, S., Beiser, A., et al., (2011). Midlife vascular risk factor exposure accelerates structural brain aging and cognitive decline. *Neurology*, 77(5), .: 461–468.
22. Dill, T. (2008). Contraindications to magnetic resonance imaging: Non-invasive imaging. *Heart*, 94(7), .: 943–948.
23. Doubal, F. N., MacLulich, A. M., Ferguson, K. J., et al., (2010). Enlarged perivascular spaces on MRI are a feature of cerebral small vessel disease. *Stroke*, 41(3), .: 450–454.
24. Durant-Fardel M. *Traite du ramollissement ducerveau (Treats softening of the brain)*. Paris, France: Balliere, 1843.
25. Etemadifar, M., Hekmatnia, A., Tayari, N., et al., (2011). Features of Virchow-Robin spaces in newly diagnosed multiple sclerosis patients. *Eur J Radiol*, 80(2), .: e104-8.
26. Fanous, R., & Midia, M. (2007). Perivascular Spaces: Normal and Giant. *Can J Neurol Sci*, 34(1), .: 5–10.
27. Fazekas, F., Chawluk, J., Alavi, A., et al., (1987). MR signal abnormalities at 1.5 T in Alzheimer’s dementia and normal aging. *Am J Roentgenol*, 149(2), .: 351–356.
28. Feigin, V. L., Roth, G. A., Naghavi, M., et al., (2016). Global burden of stroke and risk factors in 188 countries, during 1990-2013: A systematic analysis for the Global Burden of Disease Study 2013. *Lancet Neurol*, 15(9), .: 913–924.

29. Gons, R. A., van Norden, A. G., de Laat, K. F., et al., (2011). Cigarette smoking is associated with reduced microstructural integrity of cerebral white matter. *Brain*, 134(7), :. 2116–2124.
30. Groeschel, S., Chong, W. K., Surtees, R., et al., (2006). Virchow-Robin spaces on magnetic resonance images: Normative data, their dilatation, and a review of the literature. *Neuroradiology*, 48(10), :. 745–754.
31. Gutierrez, J., Elkind, M. S. V., Dong, C., et al., (2017). Brain Perivascular Spaces as Biomarkers of Vascular Risk: Results from the Northern Manhattan Study. *Am J Neuroradiol*, 38(5), :. 862–867.
32. Hara, M., Yakushiji, Y., Suzuyama, K., et al., (2019). Synergistic effect of hypertension and smoking on the total small vessel disease score in healthy individuals: The Kashima scan study. *Hypertens Res*, 42(11), :. 1738–1744.
33. Heier, L. A., Bauer, C. J., Schwartz, L., et al., (1989). Large Virchow-Robin spaces: MR-clinical correlation. *Am J Neuroradiol*, 10(5), :. 929–936.
34. Hosford, P. S., & Gourine, A. V. (2019). What is the key mediator of the neurovascular coupling response? In *Neurosci Biobehav Rev*, 96, :. 174–181.
35. Hu, X., De Silva, T. M., Chen, J., et al., (2017). Cerebral Vascular Disease and Neurovascular Injury in Ischemic Stroke. *Circ Res*, 120(3), :. 449–471.
36. Iadecola, C. (2017). The Neurovascular Unit Coming of Age: A Journey through Neurovascular Coupling in Health and Disease. *Neuron*, 96(1), :. 17–42.
37. Ihara, M., & Yamamoto, Y. (2016). Emerging Evidence for Pathogenesis of Sporadic Cerebral Small Vessel Disease. *Stroke*, 47(2), :. 554–560.

38. Issac, T. G., Chandra, S. R., Christopher, R., et al., (2015). Cerebral Small Vessel Disease Clinical, Neuropsychological, and Radiological Phenotypes, Histopathological Correlates, and Described Genotypes: A Review. *J. Geriatr.*, .: 564870.
39. Jungreis, C. A., Kanal, E., Hirsch, W. L., et al., (1988). Normal perivascular spaces mimicking lacunar infarction: MR imaging. *Radiology*, 169(1), .: 101–104.
40. Kalvach, P., Gregová, D., Skoda, O., et al., (2007). Cerebral blood supply with aging: Normal, stenotic and recanalized. *J Neurol Sci*, 257(1–2), .: 143–148.
41. Kwee, R. M., & Kwee, T. C. (2007). Virchow-Robin spaces at MR imaging. *Radiographics*, 27(4), .: 1071–1086.
42. Kynast, J., Lampe, L., Luck, T., et al., (2018). White matter hyperintensities associated with small vessel disease impair social cognition beside attention and memory. *J. Cereb. Blood Flow Metab.*, 38(6), 996–1009.
43. Li, Q., Yang, Y., Reis, C., et al., (2018). Cerebral Small Vessel Disease. *Cell Transplant.*, 27(12), .: 1711–1722.
44. Liu, J., Rutten-Jacobs, L., Liu, M., et al., (2018). Causal Impact of Type 2 Diabetes Mellitus on Cerebral Small Vessel Disease: A Mendelian Randomization Analysis. *Stroke*, 49(6), .: 1325–1331.
45. Louveau, A., Smirnov, I., Keyes, T. J., et al., (2015). Structural and functional features of central nervous system lymphatic vessels. *Nature*, 523(7560), .: 337–341.
46. Mestre, H., Kostrikov, S., Mehta, R. I., et al., (2017). Perivascular spaces, glymphatic dysfunction, and small vessel disease. *Clin Sci*, 131(17), .: 2257–2274.
47. Mitchell, G. F. (2009). Arterial Stiffness and Wave Reflection: Biomarkers of Cardiovascular Risk. *Artery Res*, 3(2), .: 56–64.

48. Monteiro, A., Castro, P., Pereira, G., et al., (2021). Neurovascular Coupling Is Impaired in Hypertensive and Diabetic Subjects Without Symptomatic Cerebrovascular Disease. *Front Aging Neurosci* 13, p. 728007.
49. Moran, C., Phan, T. G., & Srikanth, V. K. (2012). Cerebral small vessel disease: A review of clinical, radiological, and histopathological phenotypes. *Int J Stroke*, 7(1), .: 36–46.
50. Mustapha, M., Nassir, C. M. N. C. M., Aminuddin, N., et al., (2019). Cerebral Small Vessel Disease (CSVD) – Lessons From the Animal Models. *Front Physiol*, 10, .: 1317.
51. Norrving, B. (2008). Lacunar infarcts: No black holes in the brain are benign. *Pract Neurol*, 8(4), .: 222–228.
52. Oztürk, M. H., & Aydingöz, U. (2002). Comparison of MR signal intensities of cerebral perivascular (Virchow-Robin) and subarachnoid spaces. *J Comput Assist Tomogr*, 26(6), .: 902–904).
53. Pantoni, L. (2010). Cerebral small vessel disease: From pathogenesis and clinical characteristics to therapeutic challenges. *Lancet. Neurol.*, 9(7), 689–701.
54. Peng, D. (2019). Clinical practice guideline for cognitive impairment of cerebral small vessel disease. *Aging Med*, 2(2), .: 64–73).
55. Pesce, C., & Carli, F. (1988). Allometry of the perivascular spaces of the putamen in aging. *Acta Neuropathol*, 76(3), .: 292–294.
56. Plog, B., & Nedergaard, M. (2018). The Glymphatic System in Central Nervous System Health and Disease: Past, Present, and Future. *Annu Rev Pathol*, 13, .: 379-394.
57. Pollock, H., Hutchings, M., Weller, R. O., et al., (1997). Perivascular spaces in the basal ganglia of the human brain: Their relationship to lacunes. *J Anat*, 191(3), .: 337–346.

58. Potter, G. M., Chaiell, F. M., Morris, Z., et al., (2015). Cerebral perivascular spaces visible on magnetic resonance imaging: Development of a qualitative rating scale and its observer reliability. *Cerebrovasc Dis*, 39(3–4), .: 224–231.
59. Power, M. C., Tingle, J. V., Reid, et al., (2017). Midlife and Late-Life Vascular Risk Factors and White Matter Microstructural Integrity: The Atherosclerosis Risk in Communities Neurocognitive Study. *J Am Heart Assoc*, 6(5), .: e005608.
60. Presa, J. L., Saravia, F., Bagi, Z., et al., (2020). Vasculo-Neuronal Coupling and Neurovascular Coupling at the Neurovascular Unit: Impact of Hypertension. *Front Physiol*, 11, .: 584135.
61. Qu, M., Kwapong, W. R., Peng, C., et al., (2020). Retinal sublayer defect is independently associated with the severity of hypertensive white matter hyperintensity. *Brain Behav*, 10(2), p. e01521.
62. Reith, W., & Haußmann, A. (2018). Importance of Virchow-Robin spaces. *Radiologe*, 58(2), .: 142–147.
63. Renna, N. F., de Las Heras, N., & Miatello, R. M. (2013). Pathophysiology of vascular remodeling in hypertension. *Int J Hypertens*, p. 808353.
64. Román, G. C., Erkinjuntti, T., Wallin, A., Pantoni, L., & Chui, H. C. et al., (2002). Subcortical ischaemic vascular dementia. *Lancet Neurol*, 1(7), .: 426–436.
65. Rudie, J. D., Rauschecker, A. M., Nabavizadeh, S. A., & Mohan, S. (2018). Neuroimaging of Dilated Perivascular Spaces: From Benign and Pathologic Causes to Mimics. *J Neuroimaging*, 28(2), .: 139–149.
66. Sachdev, P., Kalaria, R., O'Brien, J., et al., (2014). Diagnostic criteria for vascular cognitive disorders: A VASCOG statement. *Alzheimer Dis Assoc Disord*, 28(3), .: 206–218.

67. Schwarzingner, M., Pollock, B. G., Hasan, O. S. M., et al., (2018). Contribution of alcohol use disorders to the burden of dementia in France 2008-13: A nationwide retrospective cohort study. *Lancet Public Health*, 3(3), .: e124–e132.
68. Song, C. J., Kim, J. H., Kier, E. L., et al., (2000). MR imaging and histologic features of subinsular bright spots on T2-weighted MR images: Virchow-Robin spaces of the extreme capsule and insular cortex. *Radiology*, 214(3), .: 671–677.
69. Staals, J., Makin, S. D., Doubal, F. N., et al., (2014). Stroke subtype, vascular risk factors, and total MRI brain small vessel disease burden. *Neurology*, 83(14), .: 1228–1234.
70. Thrane, V. R., Thrane, A. S., Plog, B. A., et al., (2013). Paravascular microcirculation facilitates rapid lipid transport and astrocyte signaling in the brain. *Sci. Rep.*, 3(1), 2582.
71. Van Dijk, E. J., Prins, N. D., Vrooman, H. A., et al., (2008). Progression of cerebral small vessel disease in relation to risk factors and cognitive consequences: Rotterdam Scan study. *Stroke*, 39(10), .: 2712–2719.
72. Wardlaw, J. M., Smith, C., & Dichgans, M. (2011). Mechanisms of sporadic cerebral small vessel disease: Insights from neuroimaging. *Lancet Neurol*, 12(5), .: 483–497.
73. Wardlaw, J. M., Smith, E. E., Biessels, G. J., et al., (2013). Neuroimaging standards for research into small vessel disease and its contribution to ageing and neurodegeneration. In *Lancet Neurol*, 12(8), .: 822–838.
74. Woldenberg, R. F., & Kohn, S. A. (2014). Leptomeninges; Arachnoid and Pia. M. J. Aminoff & R. B. Daroff (Eds.), *Encyclopedia of the Neurological Sciences (Second Edition)* (.: 868–871).
75. Zhang, E. T., Inman, C. B., & Weller, R. O. (1990). Interrelationships of the pia mater and the perivascular (Virchow-Robin) spaces in the human cerebrum. In *J Anat*, 170, .: 111–123.

76. Zhu, Y. C., Tzourio, C., Soumaré, A., et al., (2010). Severity of dilated Virchow-Robin spaces is associated with age, blood pressure, and MRI markers of small vessel disease: A population-based study. *Stroke*, 41(11), .: 2483–2490.
77. Zong, X., Lian, C., Jimenez, J., Yamashita, K., Shen, D., & Lin, W. et al., (2020). Morphology of perivascular spaces and enclosed blood vessels in young to middle-aged healthy adults at 7T: Dependences on age, brain region, and breathing gas. *NeuroImage*, 218, 116978.
78. Zong, X., Park, S. H., Shen, D., & Lin, W. (2016). Visualization of perivascular spaces in the human brain at 7T: sequence optimization and morphology characterization. *Neuroimage*, 125, .: 895–902.

APPENDICES

APPENDIX I: DATA COLLECTION TOOL

Study number _____

Study Group _____

Section 1: Patient Demographic and Clinical Data

Age	
Sex	
Medical history variables (medically diagnosed hypertension, diabetes, ischemic heart disease)	
Social history variables (history of smoking [indicated in pack-years], alcohol consumption [units per day])	
Clinical history (symptoms)	
Physical exam findings	

Section 2: MRI Brain Imaging Findings

<p>Potter's rating scale: 0 (no Virchow-Robin space), 1 (mild; 1–10 Virchow-Robin spaces), 2 (moderate; 11–20 Virchow-Robin spaces), 3 (frequent; 21–40 Virchow-Robin spaces) or 4 (severe; >40 Virchow-Robin spaces)</p>		
<p>Fazekas Scale</p>	<p>Periventricular (PVH, 0–3)</p>	
	<p>Deep white matter hyperintensities (dWMH, 0–3)</p>	
	<p>Total WMH burden score (0–6)</p>	
<p>Virchow-Robin space Size</p>		
<p>Virchow-Robin space Length</p>		
<p>Virchow-Robin space Width</p>		

APPENDIX II: PARTICIPANT INFORMATION AND CONSENT FORM

(To be administered in English or any other appropriate language depending on the participant's convenience e.g Kiswahili translation)

ENGLISH INFORMED CONSENT FORM

Title of Study: MAGNETIC RESONANCE ANALYSIS OF THE VIRCHOW-ROBIN SPACES
IN CEREBRAL SMALL VESSEL DISEASE

Principal Investigator and institutional affiliation:

Dr Brian Ngure Kariuki, Bsc, MBChB.

Department of Human Anatomy, University of Nairobi

Co-Investigators and institutional affiliation:

Dr Paul Odula, Bsc, MBChB, MMED (Surgery), PhD.

Senior Lecturer, Department of Human Anatomy, University of Nairobi

Prof. Obimbo Moses Madadi, MBChB, Dip FELASA C, MSc, MMED (ObGyn), PhD.

Associate Professor, Department of Human Anatomy, University of Nairobi

Dr Pamela Mandela, MBChB, MPH, MMED (ENT), PhD.

Senior Lecturer, Department of Human Anatomy, University of Nairobi

Introduction:

I would like to tell you about a study being conducted by the above-listed researchers. The purpose of this consent form is to give you the information you will need to help you decide whether or not to be a participant in the study. Feel free to ask any questions about the purpose of the research, what happens if you participate in the study, the possible risks and benefits, your rights as a volunteer, and anything else about the research or this form that is not clear. When we have answered all your questions to your satisfaction, you may decide to be in the study or not. This process is called “informed consent”. Once you understand and agree to be in the study, I will request you to sign your name on this form. You should understand the general principles which apply to all study subjects in medical research:

- i) Your decision to participate is entirely voluntary
- ii) You may withdraw from the study at any time without necessarily giving a reason for your withdrawal
- iii) Refusal to participate in the research will not affect the services you are entitled to in this health facility or other facilities. We will give you a copy of this form for your records.

May I continue? YES / NO

This study has approval by The Kenyatta National Hospital-University of Nairobi Ethics and Research Committee protocol No. _____

WHAT IS THIS STUDY ABOUT?

The researchers listed above are assessing the MRI brain scans of adults (above 18 years) of either sex (male or female) who have clinical features of cerebral small vessel disease with supporting changes on imaging as well as those whom cerebral small vessel disease has been ruled out. The purpose of the study is to find out the differences in magnetic resonance imaging features of

Virchow-Robin spaces in study subjects with and without cerebral small vessel disease. There will be approximately 108 study subjects in this study randomly chosen. We are asking for your consent to consider participating in this study.

WHAT WILL HAPPEN IF YOU DECIDE TO BE IN THIS RESEARCH STUDY?

If you agree to participate in this study, the following things will happen:

You will be asked for consent for the investigators to access and extract data from your patient hospital file on your demographics (age, sex), co-morbidities, clinical history (symptoms and physical examination findings) as well as your MRI brain scan findings.

We will ask for a telephone number where we can contact you if necessary. If you agree to provide your contact information, it will be used only by people working for this study and will never be shared with others. The reasons why we may need to contact you include: confirming details that may be missing in the file or for follow up on the progress of your condition.

ARE THERE ANY RISKS, HARMS OR DISCOMFORTS ASSOCIATED WITH THIS STUDY?

Medical research has the potential to introduce psychological, social, emotional and physical risks. Care should always be taken to minimize the risks. One potential risk of being in the study is loss of privacy. We will use a code number to identify you in a password-protected computer database and will keep all of our paper records in a locked file cabinet. However, no system of protecting your confidentiality can be secure, so it is still possible that someone could find out you were in this study and could find out information about you.

No other potential risks are associated with the aforementioned study.

ARE THERE ANY BENEFITS BEING IN THIS STUDY?

The information you provide will help us better understand the Anatomy of small vessel disease and its effects on the brain. This information is a contribution to science and could lead to early diagnosis, timely detection, as well as timely intervention in cerebral small vessel disease.

WILL BEING IN THIS STUDY COST YOU ANYTHING?

This study shall not cost you anything.

WILL YOU GET A REFUND FOR ANY MONEY SPENT AS PART OF THIS STUDY?

There are no refunds or compensation for participation in the study since you will not have any costs expended during the study.

WHAT IF YOU HAVE QUESTIONS IN FUTURE?

If you have further questions or concerns about participating in this study, please call or send a text message to the study staff at the number provided at the bottom of this page.

For more information about your rights as a research participant, you may contact the Secretary/Chairperson, Kenyatta National Hospital-University of Nairobi Ethics and Research Committee Telephone No. 2726300 Ext. 44102 email uonknh_erc@uonbi.ac.ke.

The study staff will pay you back for your charges to these numbers if the call is for study-related communication.

WHAT ARE YOUR OTHER CHOICES?

Your decision to participate in research is voluntary. You are free to decline participation in the study and you can withdraw from the study at any time without injustice or loss of any benefits.

CONSENT FORM (STATEMENT OF CONSENT)

Participant's statement

I have read this consent form or had the information read to me. I have had the chance to discuss this research study with a study counsellor. I have had my questions answered in a language that I understand. The risks and benefits have been explained to me. I understand that my participation in this study is voluntary and that I may choose to withdraw at any time. I freely agree to participate in this research study.

I understand that all efforts will be made to keep information regarding my identity confidential.

By signing this consent form, I have not given up any of the legal rights that I have as a participant in a research study.

I agree to participate in this research study: Yes No

I agree to provide contact information for follow-up: Yes No

Participant _____ **printed** _____ **name:** _____

Participant signature / Thumb stamp _____ **Date** _____

Researcher's statement

I, the undersigned, have fully explained the relevant details of this research study to the participant named above and believe that the participant has understood and has willingly and freely given his/her consent.

Researcher 's Name: _____ **Date:** _____

Signature _____

Role in the study: _____

For more information contact: Dr. Brian Ngure Kariuki; +254 715 893218

Witness Printed Name (*If witness is necessary, A witness is a person mutually acceptable to both the researcher and participant*)

Name _____ Contact information _____

Signature /Thumb stamp: _____ Date: _____

Principal Investigator's contact details:

Name: Dr Brian Ngure Kariuki **Telephone:** +254 715 893218 **Email:** kariukib88@gmail.com

Lead supervisor's contact details:

Name: Dr. Paul Odula **Telephone:** +254 722 773025, **Email:** paulodula254@gmail.com

KNH-UON-ERC contact details:

P. O. Box: 19676-00202 Nairobi **Telephone:** (254-020) 2726300-9 Ext 44355 **E-mail:** uonknh_erc@uonbi.ac.ke

Kiswahili Informed Consent Form

Kichwa cha Somo: VIPENGELE VYA MAONESHU YA UCHUNGUZI WA MAGNETIC YA NAFASI ZA VIRCHOW-ROBIN KATIKA UGONJWA WA VYOMBO VYA DUKA.

Mchunguzi Mkuu na ushirika wa taasisi:

Dkt Brian Ngure Kariuki, Bsc, MBChB.

Idara ya Anatomia ya Binadamu, Chuo Kikuu cha Nairobi

Wachunguzi-wenza na ushirika wa taasisi:

Dkt Paul Odula, Bsc, MBChB, MMED (Upasuaji), PhD.

Mhadhiri Mwandamizi, Idara ya Anatomia ya Binadamu, Chuo Kikuu cha Nairobi

Dkt Obimbo Moses Madadi, MBChB, Dip FELASA C, MSc, MMED (ObGyn), PhD.

Mhadhiri Mwandamizi, Idara ya Anatomia ya Binadamu, Chuo Kikuu cha Nairobi

Dkt Pamela Mandela, MBChB, MPH, MMED (ENT), PhD.

Mhadhiri Mwandamizi, Idara ya Anatomia ya Binadamu, Chuo Kikuu cha Nairobi

Utangulizi:

Ningependa kukuambia juu ya utafiti unaofanywa na watafiti walioorodheshwa hapo juu.

Madhumuni ya fomu hii ya idhini ni kukupa habari utakayohitaji kukusaidia kuamua ikiwa ni mshiriki wa utafiti huo au la. Jisikie huru kuuliza maswali yoyote juu ya madhumuni ya utafiti, nini kinatokea ikiwa unashiriki katika utafiti, hatari na faida zinazowezekana, haki zako kama kujitolea, na chochote kingine juu ya utafiti au fomu hii ambayo haijulikani wazi. Wakati tumejibu

maswali yako yote kukuridhisha, unaweza kuamua kuwa kwenye somo au la. Utaratibu huu unaitwa 'idhini ya habari'. Mara tu utakapoelewa na kukubali kuwa kwenye utafiti, nitakuomba utie sahihi jina lako kwenye fomu hii. Unapaswa kuelewa kanuni za jumla ambazo zinatumiwa kwa washiriki wote katika utafiti wa matibabu:

i) Uamuzi wako wa kushiriki ni wa hiari kabisa

ii) Unaweza kujiondoa kwenye utafiti wakati wowote bila kutoa sababu ya kujitoka kwako

iii) Kukataa kushiriki katika utafiti hakutaathiri huduma unazostahiki katika kituo hiki cha afya au vituo vingine. Tutakupa nakala ya fomu hii kwa kumbukumbu zako.

Naweza kuendelea? NDIO/LA

Utafiti huu umeidhinishwa na Itifaki ya Kamati ya Maadili na Utafiti ya Chuo Kikuu cha kitaifa cha Kenyatta-Chuo Kikuu cha Nairobi

UTAFITI HUU UNAHUSU NINI?

Watafiti walioorodheshwa hapo juu wanachunguza uchunguzi wa ubongo wa watu wazima (zaidi ya miaka 18) wa jinsia yoyote (wa kiume au wa kike) ambao wana huduma ya kliniki ya ugonjwa wa chombo kidogo cha ubongo na mabadiliko ya kusaidia kwenye picha na vile vile ambao ugonjwa wa chombo kidogo cha ubongo umekuwa ilitawaliwa. Madhumuni ya utafiti huo ni kujua tofauti katika huduma za upigaji picha za uwasilishaji wa nafasi za Virchow-Robin kwa wagonjwa walio na ugonjwa wa chombo kidogo na bila ubongo. Kutakuwa na takriban washiriki 108 katika utafiti huu waliochaguliwa bila mpangilio. Tunaomba idhini yako kufikiria kushiriki katika utafiti huu.

NINI KITATOKEA UKIAMUA KUWA KWENYE UTAFITI HUU WA UTAFITI?

Ikiwa unakubali kushiriki katika utafiti huu, mambo yafuatayo yatatokea:

Utaulizwa idhini kwa wachunguzi kupata na kutoa data kutoka kwa faili yako ya hospitali ya wagonjwa kwenye idadi yako ya watu (Umri, jinsia), magonjwa ya pamoja, historia ya kliniki (dalili na matokeo ya uchunguzi wa mwili) pamoja na matokeo ya uchunguzi wa ubongo wa MRI.

Tutauliza nambari ya simu ambapo tunaweza kuwasiliana nawe ikiwa ni lazima. Ikiwa unakubali kutoa habari yako ya mawasiliano, itatumiwa tu na watu wanaofanya kazi kwa utafiti huu na hawatashirikiwa na wengine kamwe. Sababu kwa nini tunaweza kuhitaji kuwasiliana na wewe ni pamoja na: kudhibitisha maelezo ambayo yanaweza kukosa kwenye faili au kwa kufuata maendeleo ya hali yako.

KUNA ATHARI ZOZOTE, ZINAZIDHARAU HASARA ZINAZOHUSIANA NA UTAFITI HUU?

Utafiti wa kimatibabu una uwezo wa kuanzisha hatari za kisaikolojia, kijamii, kihemko na kiafya. Jitihada inapaswa kuwekwa kila wakati ili kupunguza hatari. Hatari moja ya kuwa katika utafiti ni kupoteza faragha. Tutatumia nambari ya nambari kukutambulisha kwenye hifadhidata ya kompyuta inayolindwa na nywila na tutaweka rekodi zetu zote za karatasi kwenye kabati la faili lililofungwa. Walakini, hakuna mfumo wowote wa kulinda usiri wako ambao unaweza kuwa salama kabisa, kwa hivyo bado inawezekana mtu anaweza kugundua kuwa ulikuwa kwenye utafiti huu na angeweza kupata habari kukuhusu.

Hakuna hatari zingine zinazoweza kuhusishwa na utafiti uliotajwa hapo juu.

KUNA FAIDA ZOZOTE ZIKO KATIKA UTAFITI HUU?

Habari unayotoa itatusaidia kuelewa vizuri Anatomy ya ugonjwa mdogo wa chombo na athari zake kwenye ubongo. Habari hii ni mchango kwa sayansi na inaweza kusababisha utambuzi wa mapema, kugundua kwa wakati unaofaa, na pia uingiliaji wa wakati unaofaa katika ugonjwa wa chombo kidogo cha ubongo.

JE, KUWA KWENYE UTAFITI HUU KUKUGHARIMIA CHOCHOTE?

Utafiti huu hautakugarimu chochote.

JE, UTARUDISHA KWA PESA YOYOTE ILIYOTUMIWA KWA SEHEMU YA UTAFITI HUU?

Hakuna marejesho au fidia ya kushiriki katika utafiti kwani hautakuwa na gharama zozote zilizotumiwa wakati wa utafiti.

NINI KAMA UNA MASWALI BAADAYE?

Ikiwa una maswali zaidi au wasiwasi juu ya sehemu kuoga katika utafiti huu, tafadhali piga simu au tuma ujumbe mfupi kwa wafanyikazi wa utafiti kwa nambari iliyotolewa chini ya ukurasa huu.

Kwa habari zaidi juu ya haki zako kama mshiriki wa utafiti unaweza kuwasiliana na Katibu / Mwenyekiti, Hospitali ya Kitaifa ya Kenyatta-Chuo Kikuu cha Maadili na Kamati ya Utafiti ya Nairobi Nambari ya simu 2726300 Ext. Barua pepe 44102 uonknh_erc@uonbi.ac.ke.

Wafanyakazi wa utafiti watakulipa malipo yako kwa nambari hizi ikiwa simu ni ya mawasiliano yanayohusiana na utafiti.

CHAGUO ZAKO ZINGINE NI NINI?

Uamuzi wako wa kushiriki katika utafiti ni wa hiari. Uko huru kukataa kushiriki katika utafiti na unaweza kujiondoa kutoka kwa utafiti wakati wowote bila udhalimu au kupoteza faida yoyote.

FOMU YA MAJADILIANO (TAARIFA YA MAJIBU)

Taarifa ya mshiriki

Nimesoma fomu hii ya idhini au habari hiyo imesomwa kwangu. Nimekuwa na nafasi ya kujadili utafiti huu wa utafiti na mshauri wa utafiti. Nimejibiwa maswali yangu kwa lugha ambayo ninaelewa. Hatari na faida zimeelezewa kwangu. Ninaelewa kuwa ushiriki wangu katika utafiti huu ni wa hiari na kwamba ninaweza kuchagua kujiondoa wakati wowote. Ninakubali kwa hiari kushiriki katika utafiti huu wa utafiti.

Ninaelewa kuwa juhudi zote zitafanywa kutunza habari kuhusu kitambulisho changu binafsi kuwa siri.

Kwa kusaini fomu hii ya idhini, sijatoa haki yoyote ya kisheria ambayo ninayo kama mshiriki katika utafiti wa utafiti.

Ninakubali kushiriki katika utafiti huu: Ndio/Hapana

Ninakubali kutoa habari ya mawasiliano kwa ufuatiliaji: Ndio/Hapana

Jina _____ **la** _____ **Mshiriki** _____ **aliyechapishwa:** _____

Saini ya mshiriki / Stempu ya kidole gumba: _____ **Tarehe:** _____

Kauli ya mtafiti

Mimi, aliyesainiwa chini, nimeelezea kabisa maelezo yanayofaa ya utafiti huu kwa mshiriki aliyetajwa hapo juu na ninaamini kwamba mshiriki ameelewa na kwa hiari na kwa hiari ametoa idhini yake.

Jina la Mtafiti: _____ **Tarehe:** _____

Sahihi _____

Jukumu katika utafiti: _____

Kwa habari zaidi wasiliana na: Dkt Brian Ngure Kariuki; +254 715 893218

Jina Lililochapishwa la Shahidi (Ikiwa shahidi ni lazima, Shahidi ni mtu anayekubalika kwa mtafiti na mshiriki wote)

Jina _____ **Maelezo ya mawasiliano** _____

Saini / stempu ya Thumb: _____ **Tarehe:** _____

Maelezo ya mawasiliano ya Mchunguzi Mkuu:

Jina: Dkt Brian Ngure Kariuki **Simu:** +254 715 893218 **Barua pepe:** kariukib88@gmail.com

Maelezo ya mawasiliano ya msimamizi kiongozi:

Jina: Dkt Paul Odula **Simu:** +254 722 773025, **Barua pepe:** paulodula254@gmail.com

Maelezo ya mawasiliano ya KNH-UON-ERC: Sanduku la Posta: 19676-00202 **Simu ya**

Nairobi: (254-020) 2726300-9 Ext 44355 **Barua pepe:** uonknh_erc@uonbi.ac.ke

L

ORIGINALITY REPORT

10%

SIMILARITY INDEX



7%

INTERNET SOURCES

7%

PUBLICATIONS

1%

STUDENT PAPERS

PRIMARY SOURCES

1	erepository.uonbi.ac.ke:8080 Internet Source	1%
2	www.scopus.com Internet Source	1%
3	N K Rollins, C Deline, M C Morriss. "Prevalence and clinical significance of dilated Virchow-Robin spaces in childhood.", Radiology, 1993 Publication	1%
4	H. Bokura, Shotai Kobayashi, Shuhei Yamaguchi. "Distinguishing silent lacunar infarction from enlarged Virchow-Robin spaces: a magnetic resonance imaging and pathological study", Journal of Neurology, 1998 Publication	1%
5	www.science.gov Internet Source	<1%
6	www.scirp.org Internet Source	<1%
7	www.researchgate.net	